RUBBERIZED ASPHALT CONCRETE FIREBAUGH PROJECT

VOLUME 2 - LABORATORY TEST REPORT

State of California Department of Transportation
Materials Engineering and Testing Services
Office of Flexible Pavement Materials
5900 Folsom Blvd
Sacramento, California 95819

November 15, 2005

EXECUTIVE SUMMARY

The experimental overlay project located on Highway 33 near the town of Firebaugh in the central valley of California consists of nine pavement test sections with a variety of rubber-modified asphalt concrete mixes and a control section of a Type A dense-graded asphalt concrete (DGAC). The rubber-modified sections include a rubberized asphalt concrete (RAC) Type-G (wet process), a Rubber Modified Asphalt Concrete – Gap Graded (RUMAC, dry process), a Type-G Modified Binder (MB-G), and a Type-D Modified Binder (MB-D). Both the MB-G and MB-D are terminal blended wet process binders. All rubber-modified pavement test sections include two thicknesses: 45 mm and 90 mm. The DGAC section is 90 mm thick.

This report (Volume 2 of a 3 volume series) presents the results of the laboratory tests on samples obtained from the field and prepared in the laboratory. The laboratory testing program consisted of rutting and fatigue measurements as well as wheel tracking to assess moisture sensitivity. Air void content of the samples was determined prior to all testing.

Three types of samples were obtained during the construction for the performance tests: loose mix from the windrow, cores (150 mm in diameter) and slabs (440 mm x 440 mm) from the as-built pavement. The core and slab samples were taken at each end of the full-depth (90 mm) performance evaluation sections.

Cores samples were used to determine the air void content and for the rutting tests. Slab samples were used for the Hamburg wheel tracking test. Beams for fatigue testing were cut from the slab samples. The loose mix was used to determine maximum theoretical gravity and for making slabs in the lab for the Hamburg wheel tracking tests.

The rutting test was conducted in accordance with the AASHTO T320-03 test method, *Standard Method of Test for Determining the Permanent Shear Strain and Stiffness of Asphalt Mixtures Using the Superpave Shear Tester (SST)*. The frequency sweep test was conducted at 20, 40, and 60°C over a range of frequencies. Permanent shear strain was measured at 40, 50, and 60°C using a stress level of approximately 67 kPa.

The fatigue test was performed in accordance with the AASHTO T321-03 procedure, *Standard Method of Test for Determining the Fatigue Life of Compacted Hot-Mix Asphalt (HMA) Subjected to Repeated Flexural Bending*. The test was conducted at 20°C using two strain levels: approximately 400 and 600 microstrain.

The Hamburg Wheel Tracking test was performed in accordance with the AASHTO T324-04 test method, *Standard Method of Test for Hamburg Wheel-Track Testing of Compacted Hot-Mix Asphalt (HMA)*. The test has a potential to evaluate the rutting of hot-mix asphalt samples due to a weakness in the aggregate structure, inadequate binder stiffness, or moisture damage. The test was conducted on pavement cores (DGAC mix only) and field-mixed field-compacted (FMFC) and field-mixed lab-compacted (FMLC) specimens for the rubber modified mixes. The FMLC specimens were made from loose mixes obtained during the construction. All tests were conducted at 50°C.

No single mix performed best in all tests conducted. All mixes performed differently in each test. The laboratory test results indicate the following:

- The MB-D mix was the most rut resistant and the DGAC the least in the SST test.
- The MB-G mix proved to be the most fatigue resistant and the MB-D and DGAC the least in the flexural bending beam test.

- The Hamburg wheel track data indicated that the RUMAC mix was the most rut resistant; the MB-G the least. But, the RUMAC and RAC-G mixes performed best in terms of resisting moisture damage while the MB-G and MB-D mixes performed the worst.

The following conclusions can be drawn based on the overall mix performance in the laboratory tests:

- Rutting Performance - Based on the results from both the SST and Hamburg Wheel Tracking tests, the RUMAC and RAC-G were the best performers. MB-D ranked next while the MB-G and DGAC mixes were worst among the mixes tested.
- Fatigue Performance – The MB-G mix was the best performer. RAC-G and RUMAC ranked next while the MB-D and DGAC mixes were poorest among the mixes tested.
- Performance in the Hamburg Wheel Tracking Device – The RUMAC mix was the best performer. RAC-G and DGAC ranked next while the MB-G and MB-D mixes were worst among the mixes tested.

As the air void content affects the rutting performance, Caltrans should consider conducting additional SST and Hamburg wheel tracking tests on specimens made with different air void contents. The specimens can be prepared in the laboratory using available materials from the project. The test results may be useful to indicate if there is a need to revisit field density requirements during the construction.

Based on the laboratory test results, all asphalt-rubber modified mixes (except for MB-G in rutting performance) performed at least equally well as, if not better than, the conventional DGAC mix; therefore, the asphalt-rubber modified mixes should continue to be used in applications that are most cost effective.

ACKNOWLEDGEMENTS

George Cornell, Bomasur Banzon, and Sri Holikatti of Caltrans Translab conducted the air void content, rutting, and fatigue tests. Qing Lu of University of California at Berkeley conducted the Hamburg Wheel Tracking test and prepared the graphs showing the Hamburg test results.

TABLE OF CONTENTS

EXECUTIVE SUMMARY i

1.0 INTRODUCTION 1
- **1.1 BACKGROUND 1**
- **1.2 PURPOSE OF REPORT 1**
- **1.3 ORGANIZATION OF REPORT 1**

2.0 LABORATORY TESTING PROGRAM 2
- **2.1 PROPOSED LABORATORY TESTS 2**
- **2.2 MATERIALS USED 2**

3.0 RUTTING TESTS 5
- **3.1 AIR VOID CONTENT 5**
- **3.2 FREQUENCY SWEEP TEST 5**
  - *3.2.1 Test Results from Frequency Sweep Test 5*
  - *3.2.2 Shear Modulus and Phase Angle 10*
  - *3.2.3 Temperature Effect on Shear Modulus 12*
- **3.3 PERMANENT SHEAR STRAIN TEST 13**
  - *3.3.1 Test Results from Permanent Shear Strain Test 13*
  - *3.3.2 Temperature Effect on Plastic Shear Strain 17*
  - *3.3.3 Plastic Shear Strain and Air Void Content 18*
- **3.4 RELATIVE RUTTING PERFORMANCE OF MIXES 18**

4.0 FATIGUE TEST 19
- **4.1 REPEATED FLEXURAL BENDING BEAM FATIGUE TEST 19**
  - *4.1.1 Test Results from Fatigue Test 19*
  - *4.1.2 Repetitions to Failures 19*
  - *4.1.3 Initial Stiffness and Dissipated Energy 26*
- **4.2 RELATIVE FATIGUE PERFORMANCE OF MIXES 28**

5.0 HAMBURG WHEEL TRACKING TEST 29
- **5.1 FIELD-MIXED FIELD-COMPACTED CORE SAMPLES 29**
- **5.2 FIELD-MIXED FIELD-COMPACTED SLAB SPECIMENS 32**
  - *5.2.1 Test Results from FMFC Slab Specimens 32*
  - *5.2.2 Performance Comparison for FMFC Slab Specimens 35*
- **5.3 FIELD-MIXED LAB-COMPACTED SLAB SPECIMENS 36**
  - *5.3.1 Test Results from FMLC Slab Specimens 36*
  - *5.3.2 Performance Comparison for FMLC Slab Specimens 41*
- **5.4 COMPARISON OF FMFC AND FMLC SLAB SPECIMENS 42**
  - *5.4.1 Comparison of Measured Rut Depth 42*
  - *5.4.2 Effect of Air Void Content on Rutting 43*
- **5.5 RELATIVE PERFORMANCE IN HAMBURG WHEEL TRACK DEVICE 44**

6.0 CONCLUSIONS AND RECOMMENDATIONS 45
- **6.1 CONCLUSIONS 45**
- **6.2 RECOMMENDATIONS 45**

7.0 REFERENCES 46

APPENDIX A - AIR VOID CONTENT DATA

APPENDIX B - SST RUTTING TEST RESULTS

APPENDIX C - REPEATED FLEXURAL BENDING BEAM FATIGUE TEST RESULTS

APPENDIX D - HAMBURG WHEEL TRACKING TEST RESULTS

LIST OF TABLES

Table 1-1 Test Sections and Their Approximate Locations (Post Mile) 1
Table 2-1 Proposed Performance Tests for Each Mix 2
Table 2-2 Inventory of Samples Used in the Laboratory Testing 4
Table 3-1 Air Void Content Data 6
Table 3-2 Summary of Shear Modulus and Phase Angle for Frequency at 10 Hz 7
Table 3-3 Relationship between Average Shear Modulus and Test Temperature 12
Table 3-4 Summary of Plastic Shear Strain at Various Cycles 16
Table 3-5 Relative Rutting Performance Ranking 18
Table 4-1 Summary of Fatigue Test Results 25
Table 4-2 Relationships between Repetitions to Failure and Strain 26
Table 4-3 Relative Fatigue Performance Ranking 28
Table 5-1 Samples Used in Hamburg Wheel Tracking Test 29
Table 5-2 Summary of Hamburg Test Results from the Field Cores (DGAC Mix) 30
Table 5-3 Summary of Hamburg Test Results from the FMFC Slab Specimens 32
Table 5-4 Summary of Hamburg Test Results from FMLC Slab Specimens 38
Table 5-5 Relative Performance Ranking in Hamburg Wheel Track Device 44
Table 6-1 Summary of Performance Ranking 45

LIST OF FIGURES

Figure 2-1 Project Site, Layout, and Sampling Location 3
Figure 3-1 Average Complex Shear Modulus (G*) at Various Frequencies 8
Figure 3-2 Average Phase Angle at Various Frequencies 9
Figure 3-3 Comparison of Shear Modulus at Three Testing Temperatures 10
Figure 3-4 Comparison of Phase Angle at Three Testing Temperatures 11
Figure 3-5 Relationship between Shear Modulus and Phase Angle 11
Figure 3-6 Average Shear Modulus vs. Test Temperature 12
Figure 3-7 Average Plastic Shear Strain vs. Load Repetition for RAC-G Mix 13
Figure 3-8 Average Plastic Shear Strain vs. Load Repetition for RUMAC Mix 14
Figure 3-9 Average Plastic Shear Strain vs. Load Repetition for MB-G Mix 14
Figure 3-10 Average Plastic Shear Strain vs. Load Repetition for MB-D Mix 15
Figure 3-11 Average Plastic Shear Strain vs. Load Repetition for DGAC Mix 15
Figure 3-12 Comparison of Plastic Shear Strain among Mixes at Three Test Temperatures 17
Figure 3-13 Air Void Content vs. Plastic Shear Strain 18
Figure 4-1 Stiffness and Dissipated Energy vs. Number of Repetitions for RAC-G Mix 20
Figure 4-2 Stiffness and Dissipated Energy vs. Number of Repetitions for RUMAC Mix 21
Figure 4-3 Stiffness and Dissipated Energy vs. Number of Repetitions for MB-G Mix 22
Figure 4-4 Stiffness and Dissipated Energy vs. Number of Repetitions for MB-D Mix 23
Figure 4-5 Stiffness and Dissipated Energy vs. Number of Repetitions for DGAC Mix 24
Figure 4-6 Repetitions to Failure vs. Strain for All Mixes 26
Figure 4-7 Comparison of Initial Stiffness among Mixes 27
Figure 4-8 Comparison of Dissipated Energy among Mixes 27
Figure 5-1 Illustration of Various Terms Used to Analyze the Hamburg Test Results 30
Figure 5-2 Progression of Average Deformation for Cores Taken at Stat132 L1 - DGAC Mix 31
Figure 5-3 Progression of Average Deformation for Cores Taken at Stat132 L2 – DGAC Mix 31
Figure 5-4 Progression of Average Deformation for Cores Taken at Stat132 L4 – DGAC Mix 32
Figure 5-5 Progression of Average Deformation for Field Mixed Field Compacted RAC-G Mix 33
Figure 5-6 Progression of Average Deformation for Field Mixed Field Compacted RUMAC Mix 33
Figure 5-7 Progression of Average Deformation for Field Mixed Field Compacted MB-G Mix 34
Figure 5-8 Progression of Average Deformation for Field Mixed Field Compacted MB-D Mix 34
Figure 5-9 Progression of Average Deformation for Field Mixed Field Compacted DGAC Mix 35
Figure 5-10 Variation of Measured Rut Depth at 10000 and 20000 Load Cycles for FMFC Mixes 35
Figure 5-11 Comparison of Average Rut Depth for Field Mixed Field Compacted Mixes 36
Figure 5-12 Inflection Point, Inverse Creep Slope, and Inverse Stripping Slope for FMFC Mixes 37
Figure 5-13 Progression of Average Deformation for Field Mixed Lab Compacted RAC-G Mix 38
Figure 5-14 Progression of Average Deformation for Field Mixed Lab Compacted RUMAC Mix-1 39
Figure 5-15 Progression of Average Deformation for Field Mixed Lab Compacted RUMAC Mix-2 39
Figure 5-16 Progression of Average Deformation for Field Mixed Lab Compacted MB-G Mix 40
Figure 5-17 Progression of Average Deformation for Field Mixed Lab Compacted MB-D Mix 40
Figure 5-18 Variation of Measured Rut Depth at 10000 and 20000 Load Cycles for FMLC Mixes 41
Figure 5-19 Comparison of Average Rut Depth for Field Mixed Lab Compacted Mixes 41
Figure 5-20 Inflection Point, Inverse Creep Slope, and Inverse Stripping Slope for FMLC Mixes 42
Figure 5-21 Comparison of Measured Rut Depth between FMFC and FMLC Specimens 43
Figure 5-22 Measured Rut Depth vs. Air Void Content 43

1.0 INTRODUCTION

1.1 BACKGROUND

The Firebaugh study [Caltrans, 2005] is a full scale experimental overlay project located on Highway 33 near the town of Firebaugh in the central valley of California. The California Integrated Waste Management Board (CIWMB) funded this project and Caltrans developed the experimental design and specifications. The purpose of the project was to evaluate the relative field performance of various rubber modified mixes having two different layer thicknesses with conventional dense-graded asphalt concrete (DGAC) mix and to evaluate the constructability of three rubber-modified asphalt concrete mixes. The paving began in April 2004 and was completed in June 2004.

The pavement test sections include a variety of rubber-modified asphalt concrete mixes and a control section of a Type A DGAC. The rubber-modified sections include a rubberized asphalt concrete (RAC) Type-G (wet process), a Rubber Modified Asphalt Concrete – Gap Graded (RUMAC, dry process), a Type-G Modified Binder (MB-G), and a Type-D Modified Binder (MB-D). Both MB-G and MB-D are terminal blended wet process binders. The project specifications required the MB binders to have at least 15% rubber by weight of asphalt.

A total of nine test sections, as shown in Table 1-1, were constructed. Within each test section a 150-m long performance evaluation section (PES) was selected for field performance monitoring for at least five years. Companion laboratory testing was undertaken to assess the rutting and fatigue performance of the mixes.

Table 1-1 Test Sections and Their Approximate Locations (Post Mile)

Material Type	Section	Process	Thickness (mm)	Length (m)	Test Section		PES Location	
					Begin	End	Begin	End
RAC-G	1	Wet	90	300	70.956	71.143	70.985	71.080
	2		45	1000	71.143	71.764	71.391	71.486
RUMAC	3	Dry	45	1000	71.764	72.386	72.100	72.195
	4		90	700	72.386	72.821	72.495	72.590
MB-G	5	Terminal	45	1000	72.821	73.442	73.000	73.095
	6		90	700	73.442	73.877	73.500	73.595
MB-D	7	Terminal	90	700	73.877	74.312	74.055	74.150
	8		45	1000	74.312	74.934	74.500	74.595
DGAC	9	Control	90	13000	74.934	83.069	75.000	75.095

1.2 PURPOSE OF REPORT

This report presents the laboratory test results and discusses their importance. It also provides a relative ranking of the performance of the different mixes based on the laboratory test results.

1.3 ORGANIZATION OF REPORT

The lab test report has the following chapters:

- Chapter 2 provides a brief description of the laboratory test program.
- Chapters 3 through chapter 5 present the results of the rutting, fatigue, and the Hamburg Wheel Tracking tests. Also included is a discussion of the results.
- Chapter 6 provides conclusions and recommendations.

The appendices include detailed test results.

2.0 LABORATORY TESTING PROGRAM

2.1 PROPOSED LABORATORY TESTS

The proposed laboratory testing program consisted of determining the rutting and fatigue resistance of the samples as well as the performance of samples in the Hamburg wheel tracking device. Air void content of the samples was also measured prior to conducting the rutting and Hamburg wheel track test.

Table 2-1 shows the performance tests proposed and approved at several joint meetings with Caltrans, the Pavement Research Center at University of California at Berkeley and MACTEC.

Table 2-1 Proposed Performance Tests for Each Mix

Test Purpose	Sample Type (Replicate)	Material Type	Test Parameter	Test Protocol
Volumetric Properties • Bulk Specific Gravity • Maximum Theoretic Gravity	Core (2) Loose Mix	FMFC	---	CT 308 CT 309
Rutting Assessment • Stiffness • Permanent Deformation	Core (6) Core (6)	FMFC	20, 40, 60°C 40, 50, 60°C	AASHTO T 320
Fatigue Assessment	Beam (6)	FMFC	20°C (~400, 600 $\mu\varepsilon$)	AASHTO T 321
Permanent Deformation/Moisture Sensitivity	Core (8) Slab (2) Loose Mix	FMFC FMFC FMLC	50°C	AASHTO T 324

2.2 MATERIALS USED

Three types of samples were obtained during construction for the laboratory performance tests: loose mixes from windrow and cores (150 mm in diameter) and slabs (440 mm x 440 mm) from the as-built pavement. The core and slab samples were taken at each end of the full-depth (90 mm) performance evaluation sections as shown in Figure 2-1.

Cores samples were used for determining the air void content and in the rutting and Hamburg wheel tracking tests. Slab samples were used in the Hamburg wheel tracking test and also were cut into beams for the fatigue test. Loose mixes were used for determination of maximum theoretical gravity and for making slabs in the lab for the Hamburg wheel track test.

Shown in Table 2-2 is a list of samples that were used in the laboratory testing.

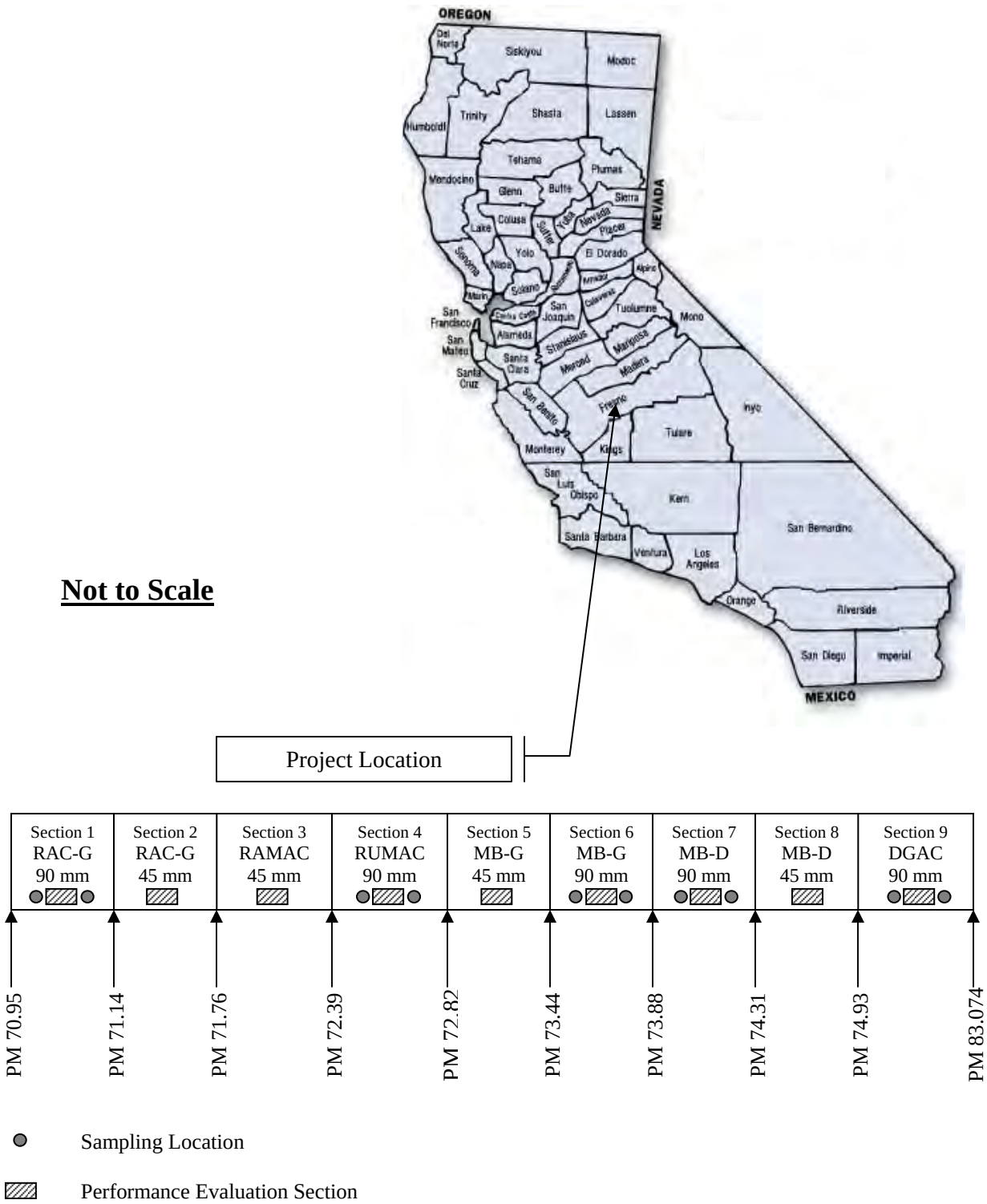

Figure 2-1 Project Site, Layout, and Sampling Location

Table 2-2 Inventory of Samples Used in the Laboratory Testing

Mix Type (PES)	Sample ID (South of PES)			Sample ID (North of PES)		
	Core for SST	Slabs		Core for SST	Slabs	
		Beams for Fatigue Test	Slab for Hamburg Test		Beams for Fatigue Test	Slabs for Hamburg Test
RAC-G (1)	01 02 03 04 05 06		2	07 08 09 10 11 12	3A 3B 4A 4B 4C 4D	3
RUMAC (4)	25 26 27 28 29 30	6B 6C 6D	6 (A, B)	31 32 33 34 35	7A 7B 7C	
MB-G (6)	43 44 45 46 47 48	10C		49 50 51 52 53 54	12A 12B 12C 12E 12F	11 2
MB-D (7)	55 56 57 58 59 60	14A 14B 14C 14D	13 14	61 62 63 64 65 66	15A 15B	
DGAC (9)*	73 74 75 76 77 78		17	79 80 81 82 83 84	19A 19B 19C 19D 20A 20B	20

*Sixteen (150-mm) DGAC cores taken at Station 132 were used for the Hamburg test and were labeled as:

L1-7, L1-8, L1-9, L1-10
L2-7, L2-8, L2-9, L2-10
L3-7, L3-8, L3-9, L3-10
L4-7, L4-8, L4-9, L4-10

3.0 RUTTING TESTS

The rut resistance of each mix was assessed in accordance with the AASHTO T320-03 [AASHTO, 2004a], *Standard Method of Test for Determining the Permanent Shear Strain and Stiffness of Asphalt Mixtures Using the Superpave Shear Tester (SST)*. This test method provides a means to determine stiffness and permanent shear strain of asphalt mixes using the Superpave Shear Tester (SST). The shear stiffness was determined following the Procedure A – Shear Frequency Sweep Test at Constant Height. The permanent shear strain was determined following the Procedure C – Repeated Shear Test at Constant Height. Prior to the rutting tests the air void content of the specimens was determined as described below.

3.1 AIR VOID CONTENT

The air void content of the samples was calculated from the bulk specific gravity (BSG) and the theoretical maximum specific gravity (G_{mm}). The bulk specific gravity was determined using the 150-mm (6-inch) cores taken from the ends of the full-depth sections in accordance with the California Test (CT) 308A procedure. The theoretical maximum specific gravity was determined using the loose mixes in accordance with the CT 309 procedure. Shown in Table 3-1 are the air void contents for samples from the five test sections. Detailed test results are presented in Appendix A.

Air void contents from south end of the PES and north end of the PES for RAC-G, RUMAC, MB-D, and DGAC sections are generally similar and the overall variation is also small. However, air void contents from the MB-G section showed 1.8% difference between that of south end (3.7%) and that of north end of the PES (1.9%). The low air void content in north end of the PES is likely due to too much asphalt or over compaction. Additional field cores may provide some insight as to the variability of the binder content.

3.2 FREQUENCY SWEEP TEST

3.2.1 Test Results from Frequency Sweep Test

Stiffness was measured at three temperatures: 20, 40, and 60°C over a range of frequencies. A summary of shear modulus and phase angle for the test frequency of 10 Hz is shown in Table 3-2. The test results, complex shear modulus and phase angle at various frequencies, are illustrated in Figures 3-1 and 3-2, respectively.

The general trend is that the shear modulus (G*) increases with the testing frequency. For the same testing frequency, the shear modulus increases as testing temperature decreases. All mixes exhibit the same characteristics. The MB mixes generally had lower shear moduli compared to other mixes. DGAC had the highest shear moduli at 20°C; RAC-G and RUMAC had higher shear moduli than MB and DGAC mixes at 60°C. There is no obvious relationship between phase angle and testing frequency.

Table 3-1 Air Void Content Data

Mix (PES)	South End of PES		North End of PES		Overall Air Voids, %
	Core ID	Air Voids, %	Core ID	Air Voids, %	
RAC-G (1)	01	6.2	07	6.4	
	02	7.4	08	7.5	
	03	5.8	09	6.5	
	04	6.9	10	8.0	
	05	6.2	11	6.5	
	06	7.3	12	8.0	
	Mean	**6.6**		**7.1**	**6.9**
	Std. Dev.	**0.7**		**0.8**	**0.7**
	CV, %	**10**		**11**	**11**
RUMAC (4)	25	3.9	31	4.9	
	26	4.4	32	4.5	
	27	5.7	33	3.7	
	28	4.7	34	4.2	
	29	5.6	35	5.1	
	30	3.8			
	Mean	**4.7**		**4.5**	**4.6**
	Std. Dev.	**0.8**		**0.6**	**0.7**
	CV, %	**17**		**12**	**15**
MB-G (6)	43	3.3	49	1.2	
	44	4.1	50	2.7	
	45	3.5	51	1.8	
	46	4.2	52	2.3	
	47	3.3	53	1.7	
	48	4.1	54	1.8	
	Mean	**3.7**		**1.9**	**2.8**
	Std. Dev.	**0.4**		**0.5**	**1.1**
	CV, %	**11**		**27**	**37**
MB-D (7)	55	3.4	61	3.2	
	56	4.1	62	4.0	
	57	3.9	63	3.8	
	58	3.9	64	3.8	
	59	3.7	65	3.1	
	60	4.4	66	3.6	
	Mean	**3.9**		**3.6**	**3.7**
	Std. Dev.	**0.3**		**0.4**	**0.4**
	CV, %	**8**		**10**	**10**
DGAC (9)	73	6.1	79	7.3	
	74	6.9	80	6.3	
	75	5.4	81	7.2	
	76	7.1	82	6.8	
	77	5.3	83	7.0	
	78	6.9	84	6.5	
	Mean	**6.3**		**6.8**	**6.6**
	Std. Dev.	**0.8**		**0.4**	**0.7**
	CV, %	**13**		**6**	**10**

Table 3-2 Summary of Shear Modulus and Phase Angle for Frequency at 10 Hz

Mix (PES)	Of PES	Core ID	Air Voids, %	Test Temp, °C	Phase Angle	G*, MPa
RAC-G (1)	South	RCG01_40	6.2	40	35.0	254.1
		RCG02_40	7.4	40	39.6	195.6
		RCG05_60	6.2	60	37.8	128.3
	North	RCG07_60	6.4	60	38.8	87.5
		RCG11_20	6.5	20	19.8	1108.2
		RCG12_20	8.0	20	19.8	1108.1
RUMAC (4)	South	RMG25_40	3.9	40	19.4	1808.5*
		RMG26_40	4.4	40	30.5	92.7*
		RMG29_60	5.6	60	39.9	72.2
		RMG30_60	3.8	60	18.9	182.2
	North	RMG34_20	4.2	20	23.0	1336.3
		RMG35_20	5.1	20	23.3	1147.7
MB-G (6)	South	MBG44_60	4.1	60	33.7	41.1
		MBG45_60	3.5	60	24.6	65.2
		MBG47_20	3.3	20	42.4	835.5
	North	MBG51_40	1.8	40	51.4	119.3
		MBG53_40	1.7	40	59.9	90.7
MB-D (7)	South	MBD55_40	3.4	40	45.5	163.7
		MBD56_40	4.1	40	45.2	151.1
		MBD59_60	3.7	60	32.8	50.5
		MBD60_60	4.4	60	35.3	55.1
	North	MBD65_20	3.1	20	30.9	1322.4
		MBD66_20	3.6	20	34.4	1205.7
DGAC (9)	South	DGA73_40	6.1	40	41.5	79.2
		DGA75_40	5.4	40	35.9	391.9
		DGA77_60	5.3	60	41.0	73.4
		DGA78_60	6.9	60	41.0	101.2
	North	DGA83_20	7.0	20	22.8	1478.6
		DGA84_20	6.5	20	22.9	1435.5

* The results are questionable due to a large difference in the G* value.

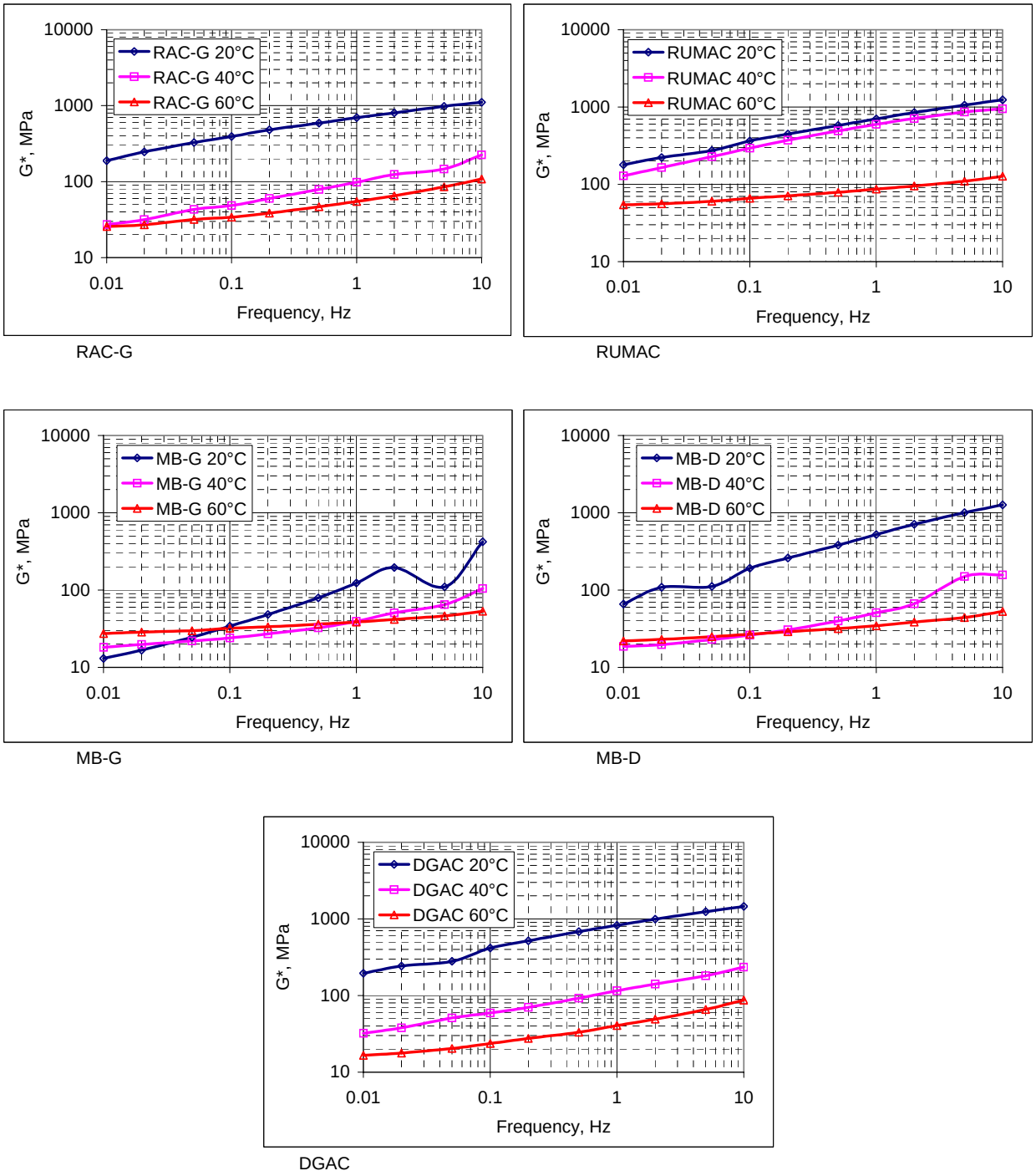

Figure 3-1 Average Complex Shear Modulus (G*) at Various Frequencies

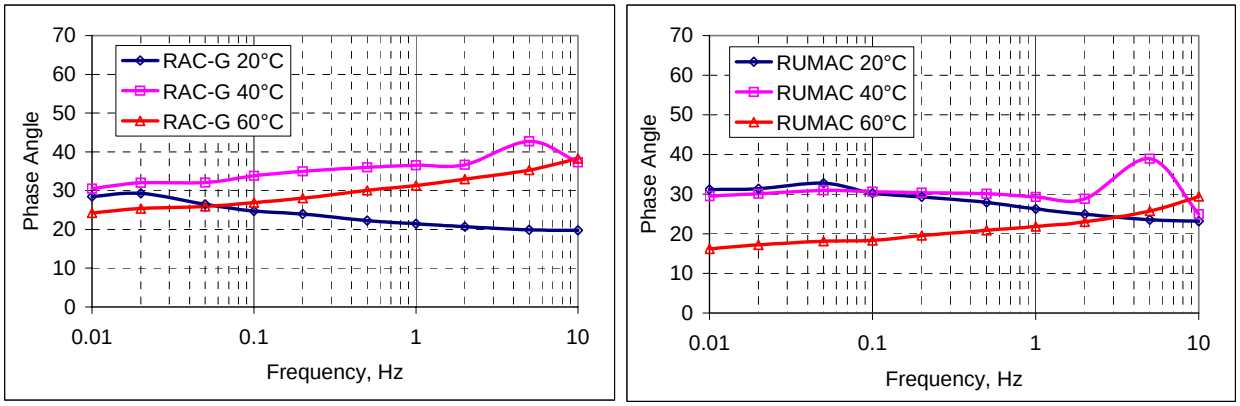

RAC-G

RUMAC

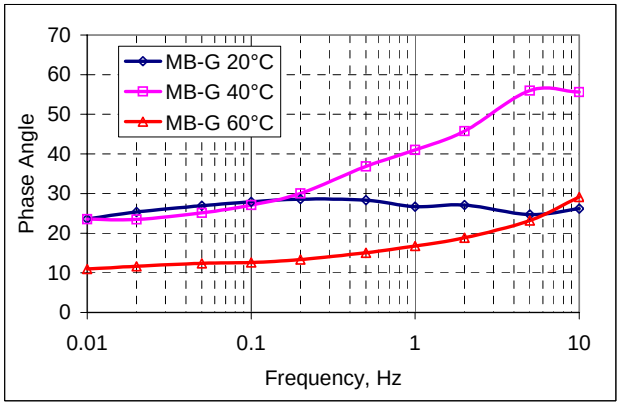

MB-G

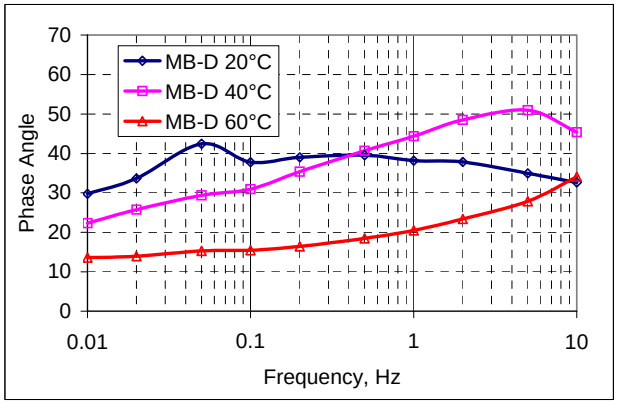

MB-G

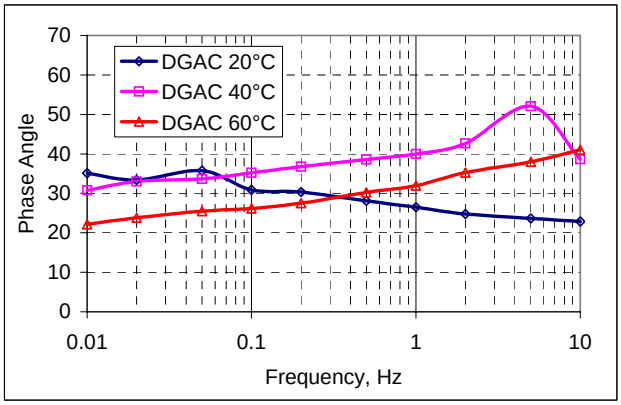

DGAC

Figure 3-2 Average Phase Angle at Various Frequencies

3.2.2 Shear Modulus and Phase Angle

Figure 3-3 shows shear moduli as a function of test temperature. The figure indicates that at the lower temperature (20°C), the variation in shear moduli is much smaller than that at higher temperatures.

Shown in Figure 3-4 is phase angle as a function of test temperature. It appears that for the RAC-G, RUMAC, and DGAC mixes the phase angle values are related to the test temperature: a lower testing temperature would result in a smaller phase angle. For the MB-G and MB-D mixes this trend is not evident.

A relationship between shear modulus and phase angle is shown in Figure 3-5. It appears that shear modulus is generally inversely related to phase angle, that is, a mix with smaller phase angle exhibits a higher shear modulus.

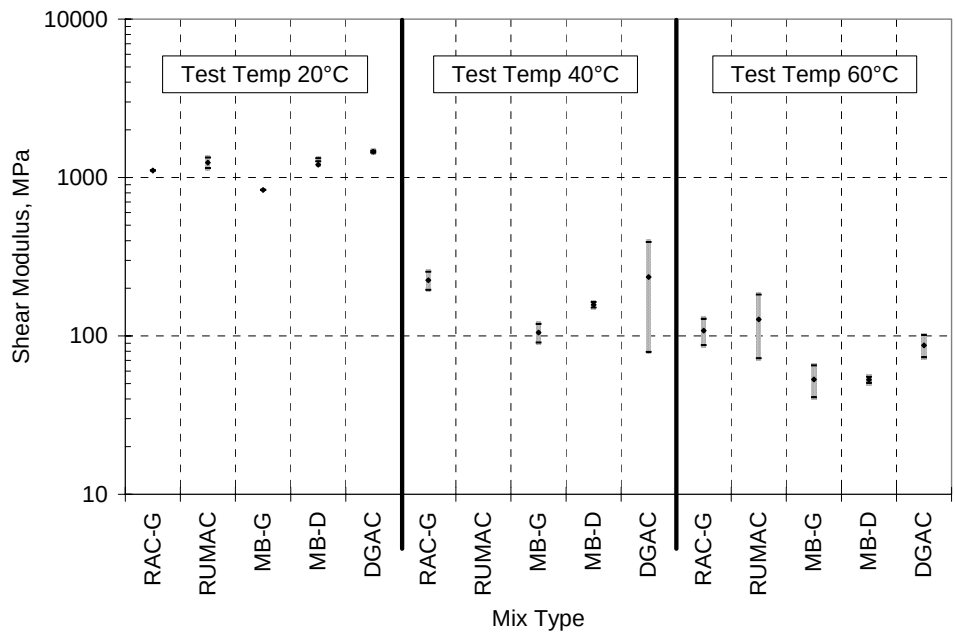

Figure 3-3 Comparison of Shear Modulus at Three Testing Temperatures

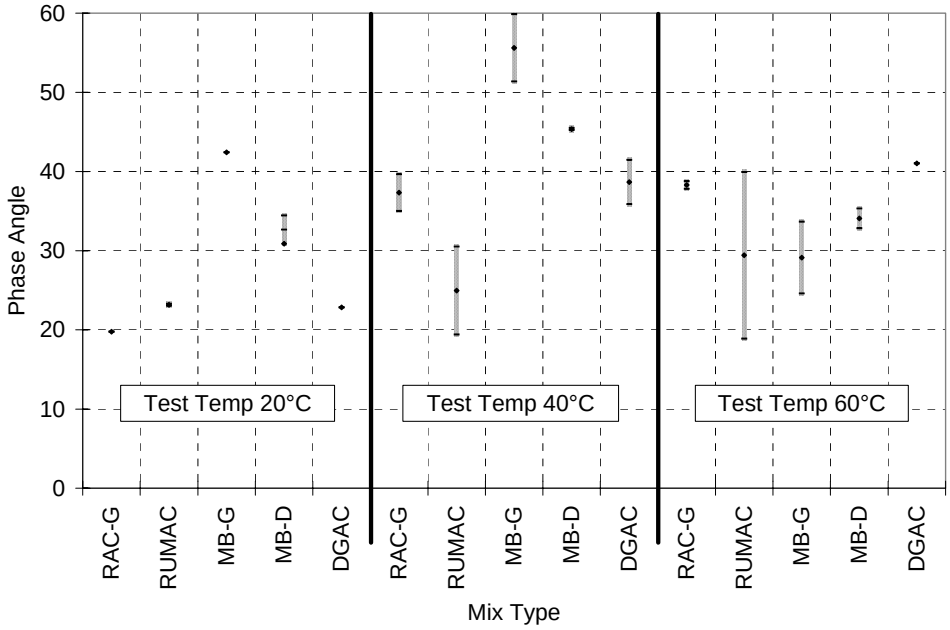

Figure 3-4 Comparison of Phase Angle at Three Testing Temperatures

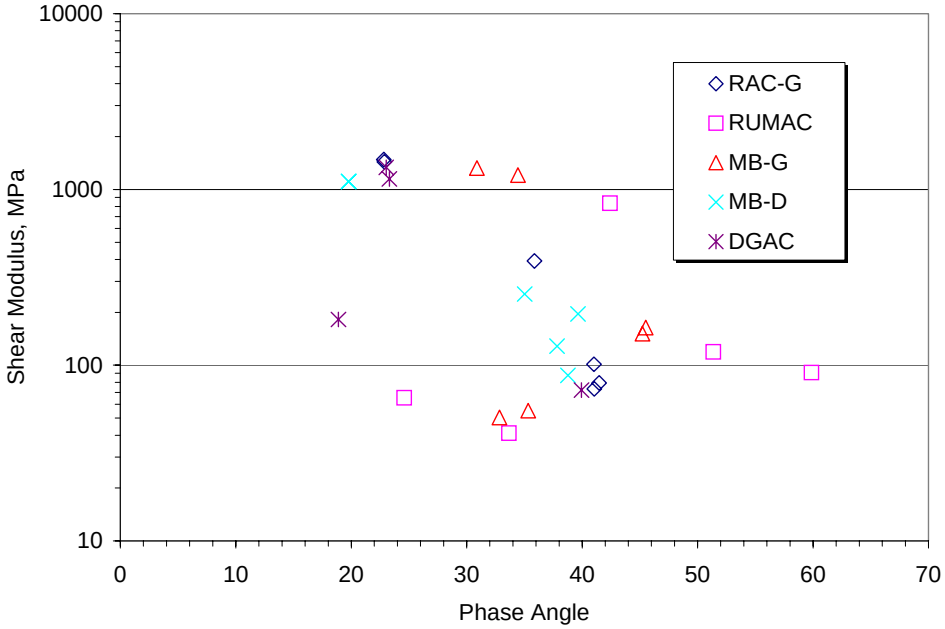

Figure 3-5 Relationship between Shear Modulus and Phase Angle

3.2.3 Temperature Effect on Shear Modulus

A relationship between average shear modulus and test temperature is illustrated in Figure 3-6. As expected, shear modulus for all mixes is a function of temperature: the higher the testing temperature, the lower the shear modulus. The figure indicates that MB-G has the lowest shear modulus compared to other mixes regardless of test temperature. Regression equations relating test temperature to shear modulus are presented in Table 3-3. All mixes show a high degree of correlation between test temperature and shear modulus.

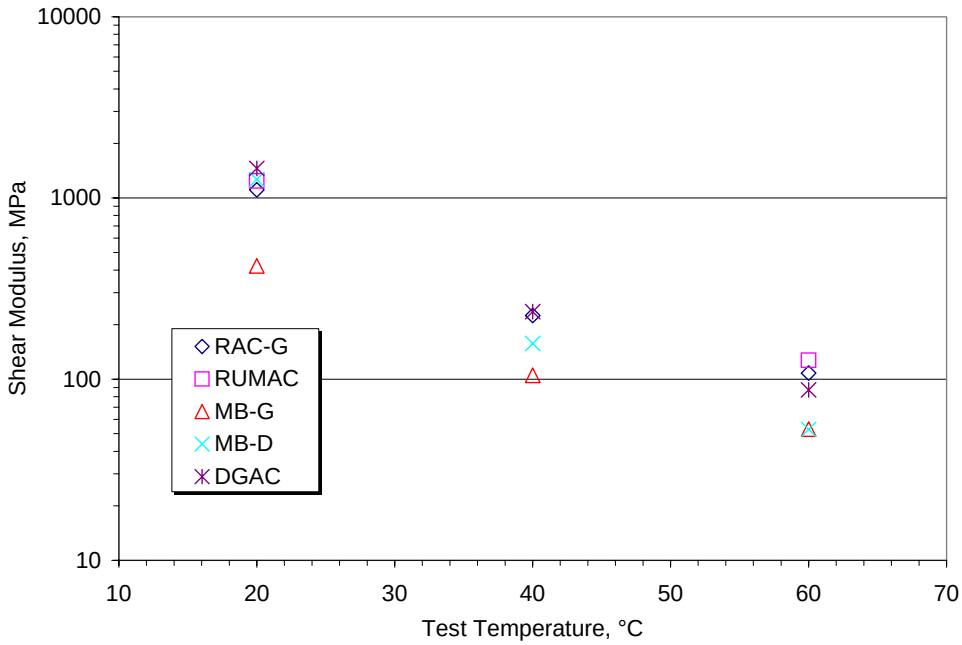

Figure 3-6 Average Shear Modulus vs. Test Temperature

Table 3-3 Relationship between Average Shear Modulus and Test Temperature

Mix Type	Shear Modulus as a Power Function of Testing Temperature (x)	R^2
RAC-G	$653670x^{-2.1397}$	0.9964
RUMAC	$620213x^{-2.0741}$	1.0000*
MB-G	$123151x^{-1.9009}$	0.9979
MB-D	$7406417x^{-2.9025}$	0.9992
DGAC	$3171886x^{-2.5693}$	0.9997

* Two data points only. Data @ 40°C was questionable; therefore, it was excluded.

3.3 PERMANENT SHEAR STRAIN TEST

3.3.1 Test Results from Permanent Shear Strain Test

A stress-controlled (67 kPa) test, the load was applied for 0.1 seconds with a 0.6 second rest between load pulses. The loading was repeated for 45,000 repetitions or until 5% shear strain was accumulated. The testing was performed at 40, 50, and 60°C.

Figures 3-7 through 3-11 illustrate average plastic shear strain at each test temperature versus load repetitions for the RAC-G, RUMAC, MB-G, MB-D, and DGAC mixes, respectively. As expected, and as shown here, the accumulation of plastic shear strain is proportional to test temperature. Permanent plastic shear strains at load repetitions of 1000, 5000, 10000, 20000, and 45000 are summarized in Table 3-4. Detailed test results for each sample are provided in Appendix B.

The effect of test temperature and air void content on plastic shear strain is discussed in greater detail in the following sections.

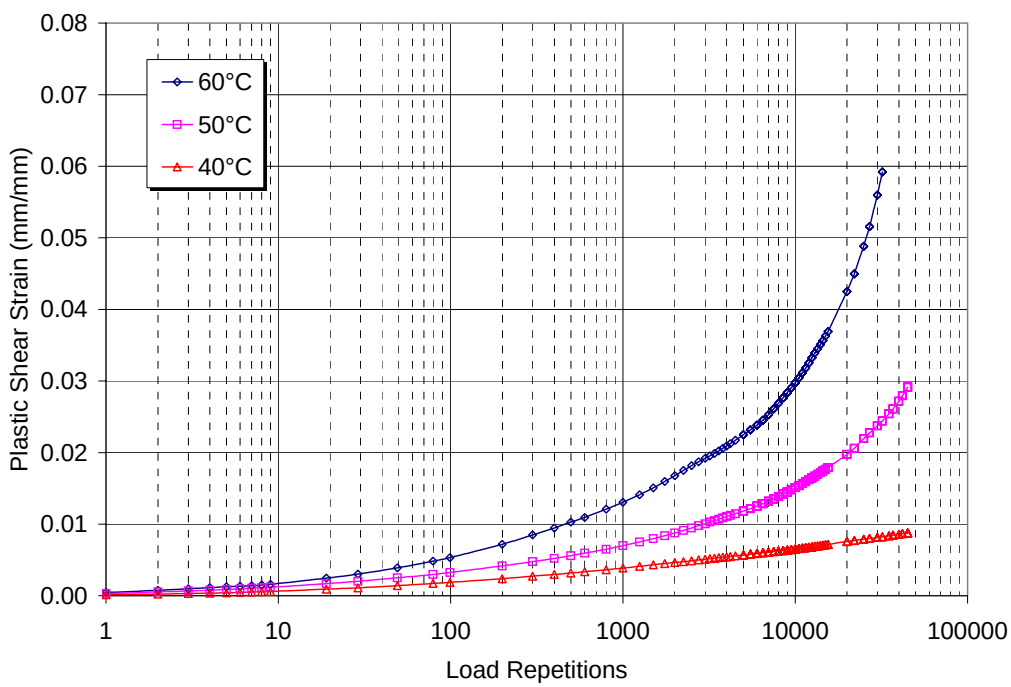

Figure 3-7 Average Plastic Shear Strain vs. Load Repetition for RAC-G Mix

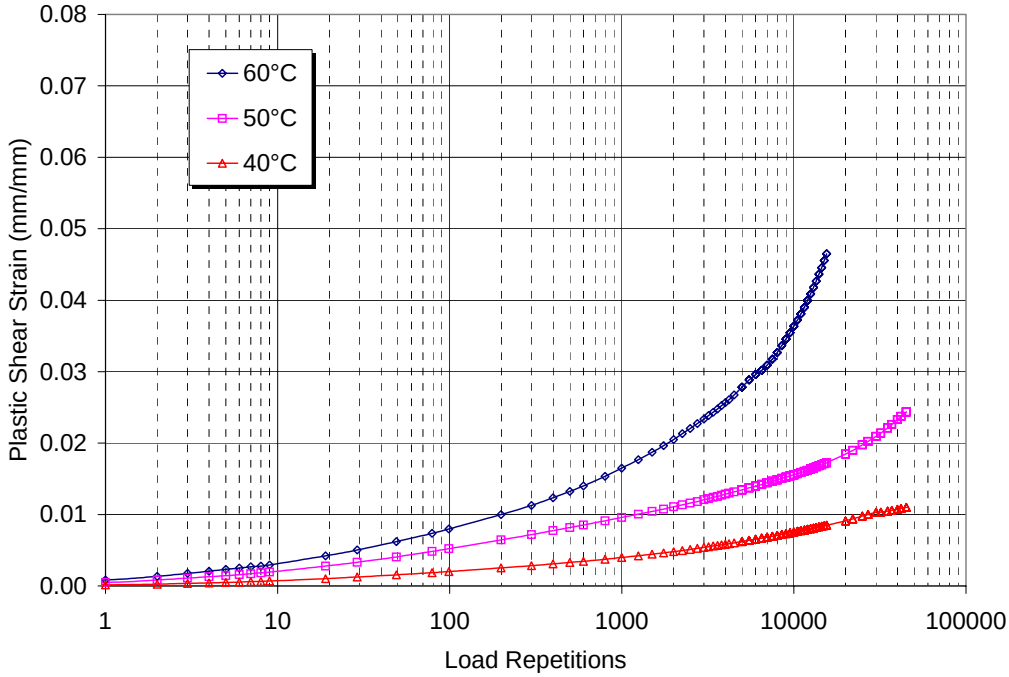

Figure 3-8 Average Plastic Shear Strain vs. Load Repetition for RUMAC Mix

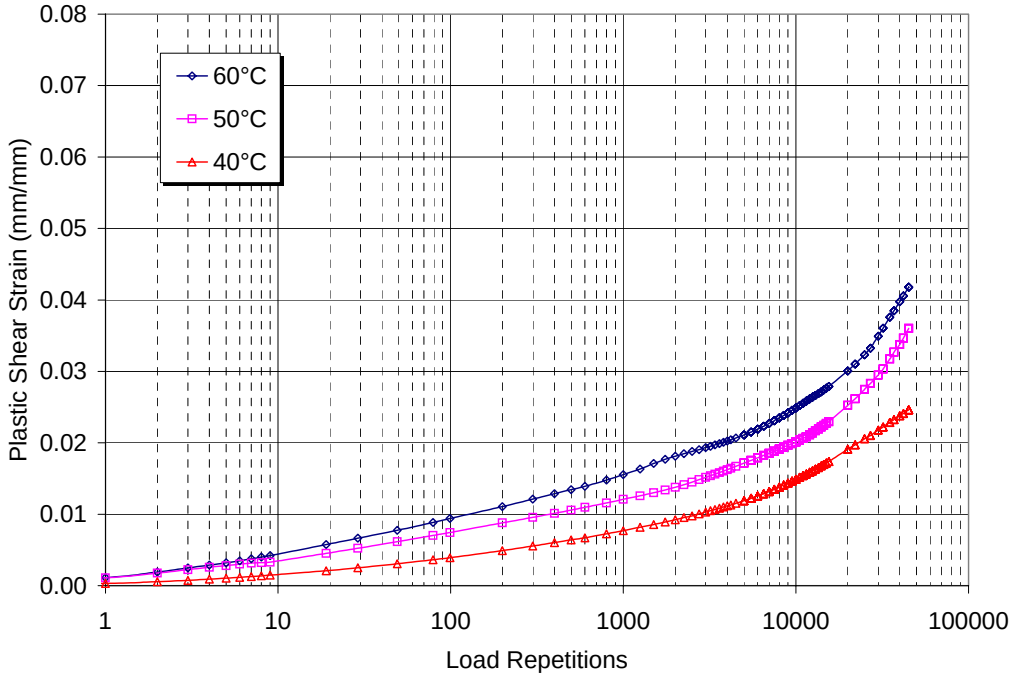

Figure 3-9 Average Plastic Shear Strain vs. Load Repetition for MB-G Mix

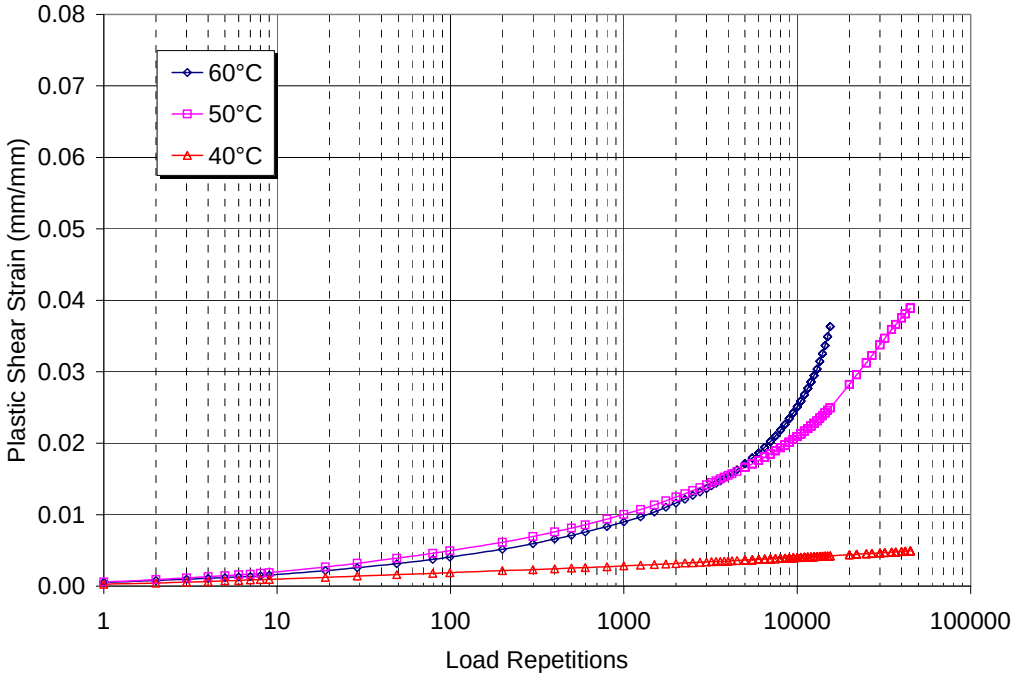

Figure 3-10 Average Plastic Shear Strain vs. Load Repetition for MB-D Mix

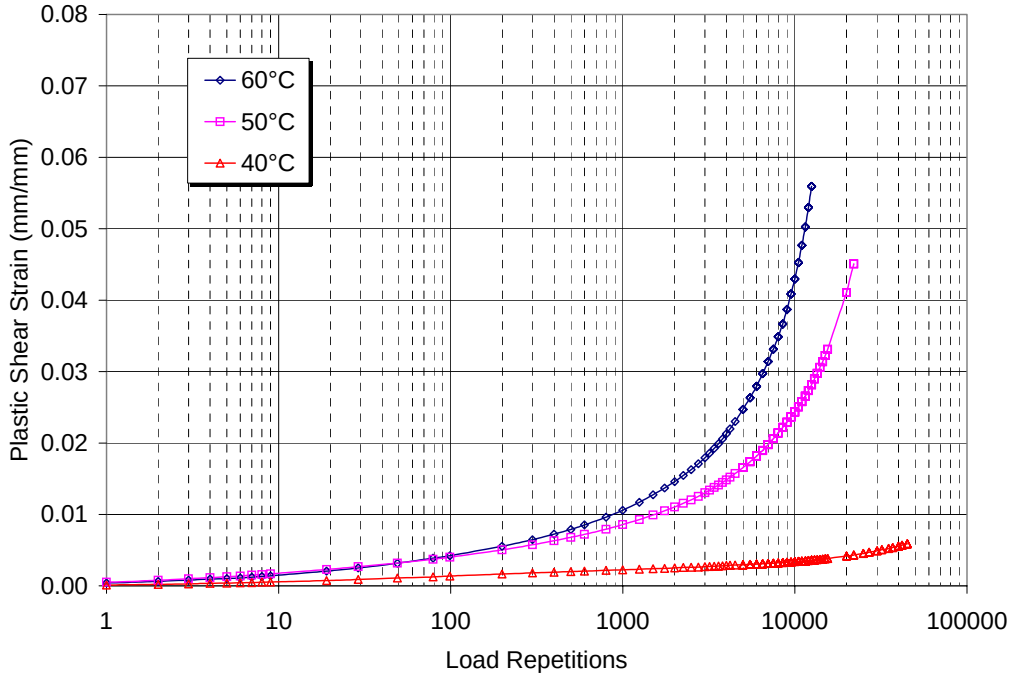

Figure 3-11 Average Plastic Shear Strain vs. Load Repetition for DGAC Mix

Table 3-4 Summary of Plastic Shear Strain at Various Cycles

Mix (PES)	Of PES	Core ID	Air Voids, %	Test Temp, °C	1000	5000	10000	20000	45000
RAC-G (1)	South	RCG01R40	6.2	40	0.003194	0.004766	0.005515	0.006410	0.007715
		RCG02R40	7.4	40	0.006467	0.009821	0.011486	0.013513	0.016095
		RCG03R40	5.8	40	0.001949	0.002509	0.002558	0.002802	0.002558
	North	RCG07R60	6.4	60	0.013683	0.023644	0.030922	0.046153	>0.05
		RCG08R60	7.5	60	0.012425	0.021357	0.028590	0.038856	0.055507
		RCG09R50	6.5	50	0.007011	0.011822	0.015086	0.019728	0.029133
RUMAC (4)	South	RMG25R40	3.9	40	0.001333	0.002297	0.002717	0.003013	0.003631
		RMG26R40	4.4	40	0.002774	0.004135	0.005051	0.007057	0.008195
		RMG27R40	5.7	40	0.007599	0.012129	0.014926	0.017649	0.021783
		RMG28R40	4.7	40	0.004216	0.006299	0.007490	0.008780	0.010392
	North	RMG31R60	4.9	60	0.016880	0.031189	0.043146	>0.05	>0.05
		RMG32R60	4.5	60	0.016104	0.024480	0.029575	0.036782	0.048414
		RMG33R50	3.7	50	0.009099	0.013315	0.015387	0.017902	0.022118
		RMG34R50	4.2	50	0.010064	0.013558	0.015724	0.019021	0.026576
MB-G (6)	South	MBG46R50	4.2	50	0.010041	0.015904	0.019524	0.026690	0.043413
		MBG47R50	3.3	50	0.014123	0.018419	0.020700	0.023807	0.028637
	North	MBG49R60	1.2	60	0.026301	0.032769	0.036960	0.043016	0.055031
		MBG50R60	2.7	60	0.004789	0.009406	0.012816	0.017143	0.028555
		MBG52R40	2.3	40	0.005933	0.007788	0.008716	0.009717	0.010913
		MBG53R40	1.7	40	0.009461	0.016005	0.021103	0.028457	0.038359
MB-D (7)	South	MBD55R40	3.4	40	0.002346	0.003030	0.003298	0.003518	0.003884
		MBD56R40	4.1	40	0.003101	0.003902	0.004266	0.004655	0.005189
		MBD57R40	3.9	40	0.003326	0.004316	0.004702	0.005184	0.005763
		MBD58R40	3.9	40	0.002538	0.003360	0.003770	0.004206	0.004858
		MBD59R60	3.7	60	0.009204	0.015817	0.019814	0.025773	0.041955
		MBD60R60	4.4	60	0.010416	0.023739	0.039703	>0.05	>0.05
	North	MBD61R60	3.2	60	0.007257	0.011844	0.015704	0.020922	>0.05
		MBD63R50	3.8	50	0.004891	0.008088	0.010002	0.013514	0.020128
		MBD64R50	3.8	50	0.015186	0.025118	0.031828	0.042898	0.057675
DGAC (9)	South	DGA73R40	6.1	40	0.002173	0.003408	0.004199	0.005236	0.006941
		DGA75R40	5.4	40	0.002033	0.002678	0.002728	0.002629	Stopped
		DGA76R40	7.1	40	0.002525	0.002773	0.003268	0.004629	0.008491
		DGA77R60	5.3	60	0.010186	0.021186	0.032973	0.071927	>0.05
		DGA78R60	6.9	60	0.011290	0.027243	0.045020	>0.05	>0.05
	North	DGA79R60	7.3	60	0.018245	>0.05	>0.05	>0.05	>0.05
		DGA80R60	6.3	60	0.010251	0.025692	0.050917	>0.05	>0.05
		DGA81R50	7.2	50	0.010991	0.022651	0.033691	0.058595	>0.05
		DGA82R50	6.8	50	0.006174	0.010490	0.014980	0.023513	0.067020

3.3.2 Temperature Effect on Plastic Shear Strain

Figure 3-12 shows permanent plastic shear strains at various load applications. Note that the mix performance varies somewhat with temperature. At 40°C, the MB-G mix had the highest plastic shear strain. At 50°C, the MB-G, MB-D, and DGAC mixes had higher plastic shear strains than those of RAC-G and RUMAC mixes. At 60°C, the DGAC mix had the highest plastic shear strain.

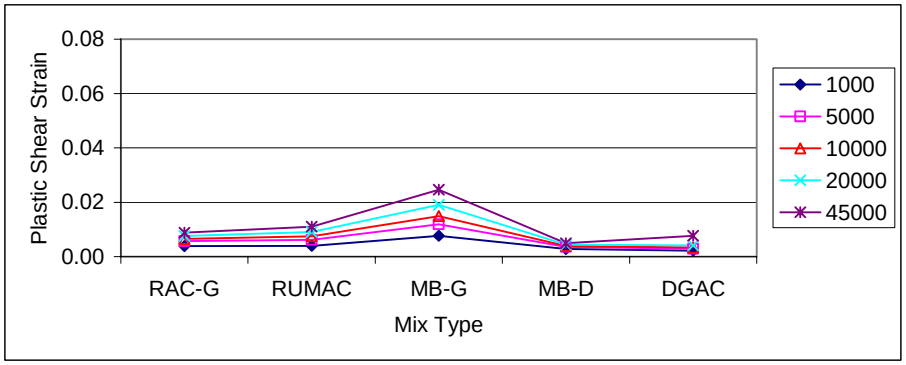

Test Temperature 40°C

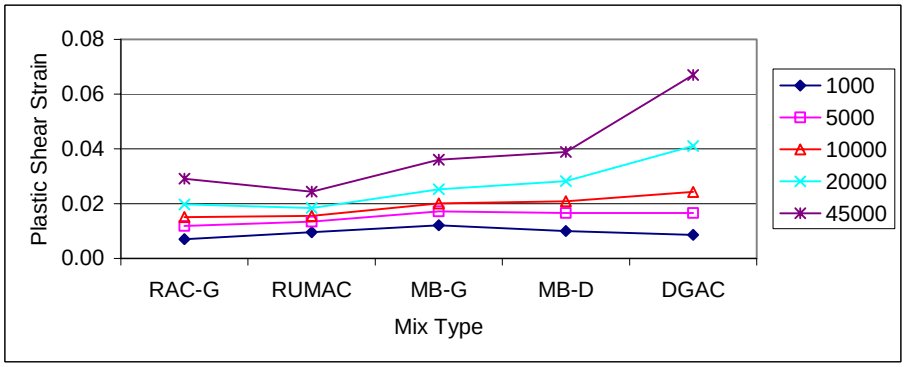

Test Temperature 50°C

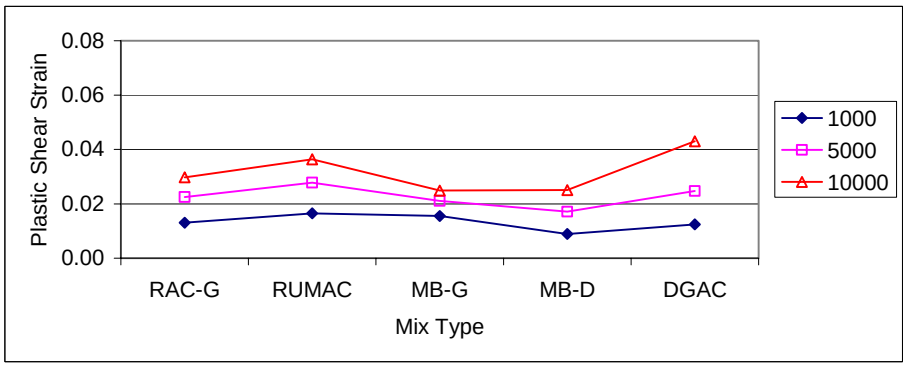

Test Temperature 60°C

Figure 3-12 Comparison of Plastic Shear Strain among Mixes at Three Test Temperatures

3.3.3 Plastic Shear Strain and Air Void Content

A relationship between air void content and plastic shear strain is shown in Figure 3-13. The figure indicates that the plastic shear strain is significantly affected by the air void content. For the RUMAC, MB-D, and DGAC mixes, the plastic shear strain increased as the air void content increased. This is apparent at both 40 and 60°C. For the RAC-G mix, the plastic shear strain increased with increasing air void content at 40°C, but slightly decreased with increasing the air void content at 60°C. For the MB-G mix, the plastic shear strain increased with decreasing air void content. Bleeding in the MB-G sections was observed in the field [MACTEC, 2005]; presumably, it is related to the extremely low void content.

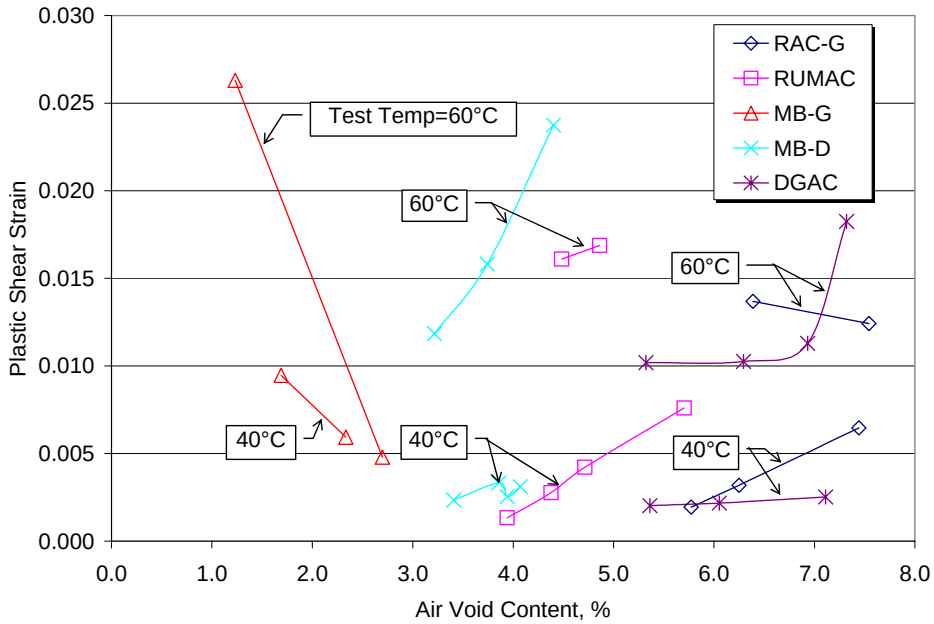

Figure 3-13 Air Void Content vs. Plastic Shear Strain

3.4 RELATIVE RUTTING PERFORMANCE OF MIXES

A simple method was used to rank the relative performance of the mixes. The method is based on a 1-5 scale with 5 being the best. Table 3-5 provides a summary of this ranking for each mix type. The summary indicates the rutting performance of the mixes is influenced by the test temperature. Overall, the MB-D mix had the highest total score, indicating the mix was generally the best in rutting performance. The RUMAC and RAC-G mixes ranked next while the MB-G and DGAC mixes were worst among the mixes tested. In the June 2005 field survey none of the mixes exhibited any significant rutting.

Table 3-5 Relative Rutting Performance Ranking

Mix Type	Performance Ranking @			Total Score
	40°C	50°C	60°C	
RAC-G	3	4	3	10
RUMAC	2	5	2	9
MB-G	1	3	4	8
MB-D	5	2	5	12
DGAC	4	1	1	6

4.0 FATIGUE TEST

The fatigue test was performed in accordance with the AASHTO T321-03 procedure [AASHTO, 2004b], *Standard Method of Test for Determining the Fatigue Life of Compacted Hot-Mix Asphalt (HMA) Subjected to Repeated Flexural Bending*. In this strain-controlled test procedure failure is defined as the load cycle at which the specimen exhibits a 50% reduction in stiffness relative to the initial stiffness.

4.1 REPEATED FLEXURAL BENDING BEAM FATIGUE TEST

The repeated flexural bending beam fatigue test was performed at two strain levels: approximately 400 and 600 microstrain. These strain levels were selected to ensure a minimum 10,000 loading cycles with failure in a reasonable amount of time. All testing was performed at 20°C at a frequency of 10 Hz.

4.1.1 Test Results from Fatigue Test

Figures 4-1 through 4-5 show the changes in average stiffness and dissipated energy during the test. Test results for each sample are provided in Appendix C. The results indicate that both stiffness and dissipated energy decrease with increasing load repetitions.

Further, test temperature can have considerable effect on the stiffness and repetitions to failure. This can be seen from specimen MBG12B (in appendix C) where the initial stiffness of the sample was measured at temperature 21.7°C (proposed testing temperature was 20°C). At 25000 repetitions the test temperature reached 21.9°C. An adjustment was made and the test temperature began to decrease. At 50000 repetitions, the test temperature had reduced to 20.2°. This change in temperature (although only 1.7°C) had a significant effect on the stiffness and the number of repetitions to failure.

4.1.2 Repetitions to Failures

Table 4-1 summarizes the initial stiffness, phase angles, and number of cycles to failure data. Figure 4-6 shows the relationship between repetitions to failure and strain for all five mixes tested. The figure indicates that the MB-G mix is the most resistant to fatigue, the DGAC mix the least.

The repetitions to failure and strain relationship may be expressed in an exponential function as shown in Table 4-2. Note that these relationships are specific to the specimens tested. Caution must be exercised when using these relationships for other mix types.

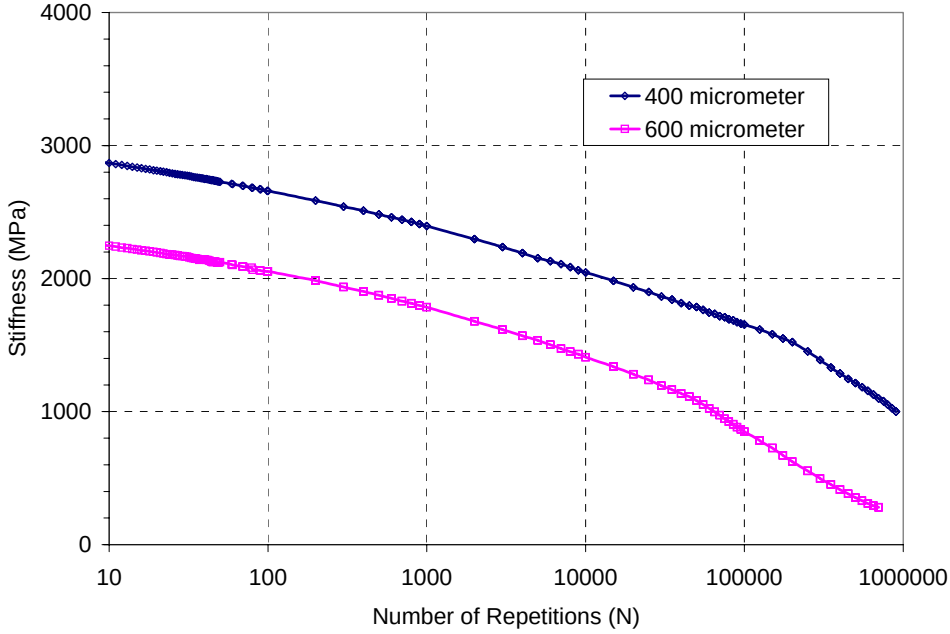

a) Stiffness

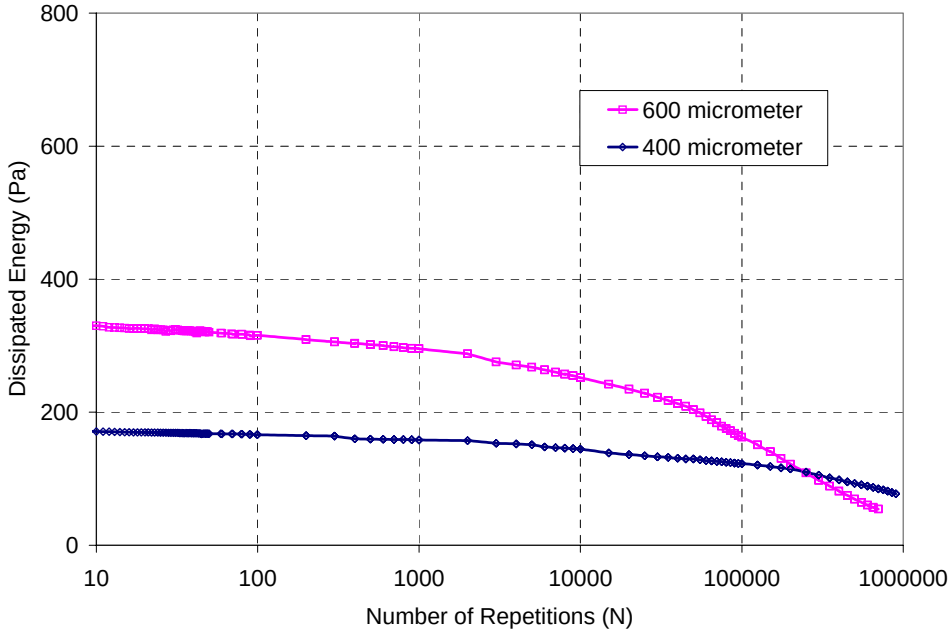

b) Dissipated Energy

Figure 4-1 Stiffness and Dissipated Energy vs. Number of Repetitions for RAC-G Mix

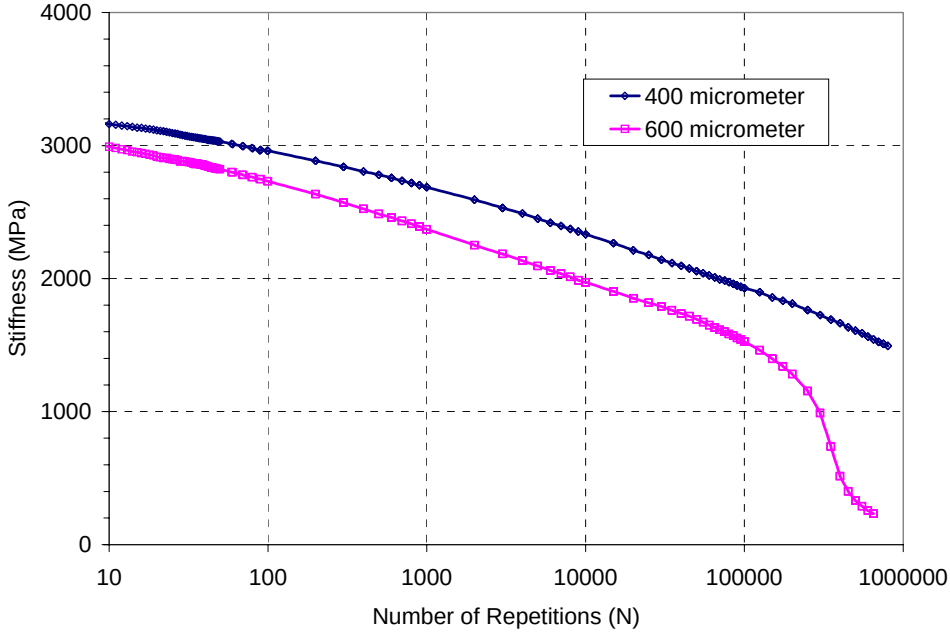

a) Stiffness

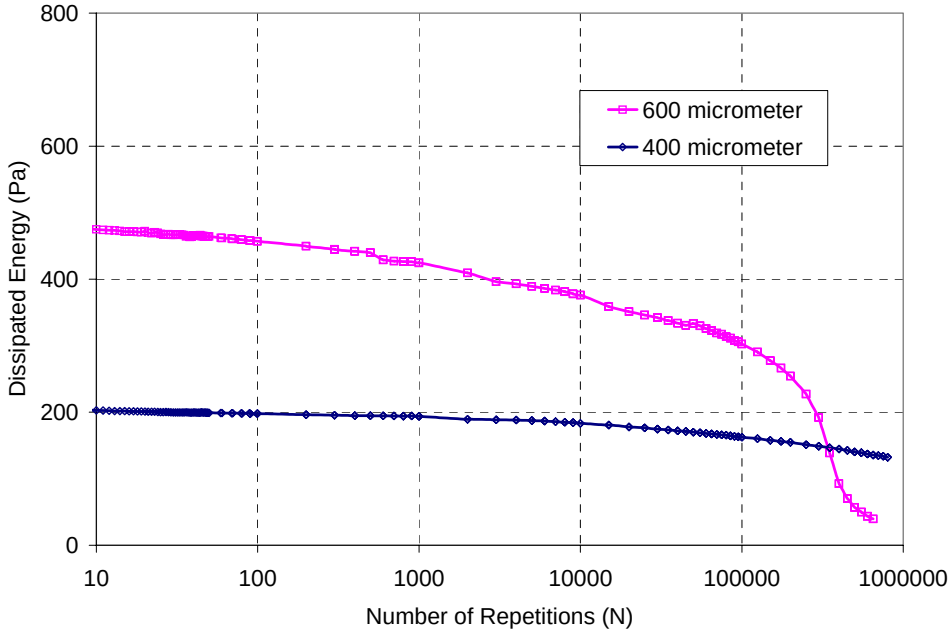

b) Dissipated Energy

Figure 4-2 Stiffness and Dissipated Energy vs. Number of Repetitions for RUMAC Mix

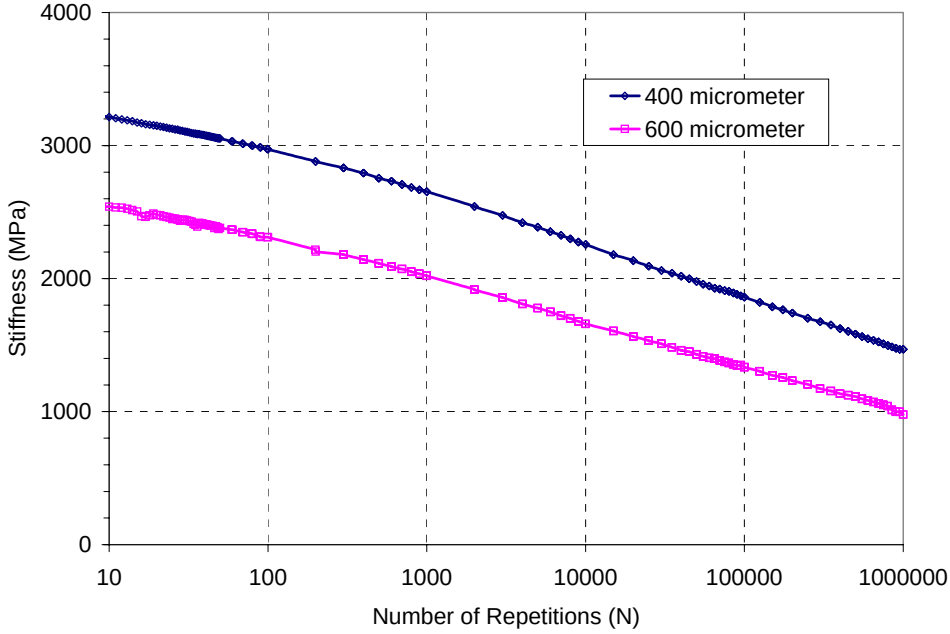

a) Stiffness

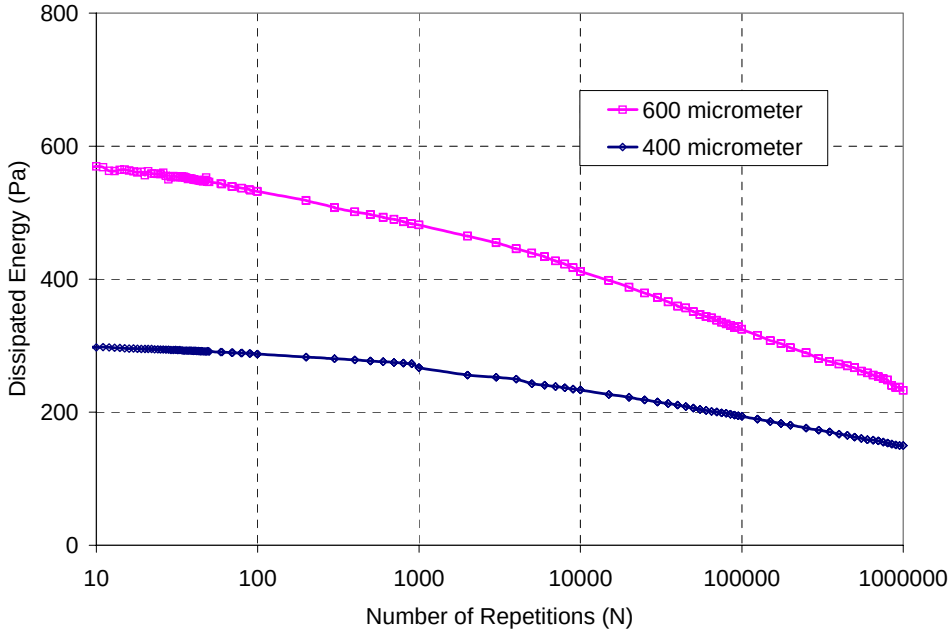

b) Dissipated Energy

Figure 4-3 Stiffness and Dissipated Energy vs. Number of Repetitions for MB-G Mix

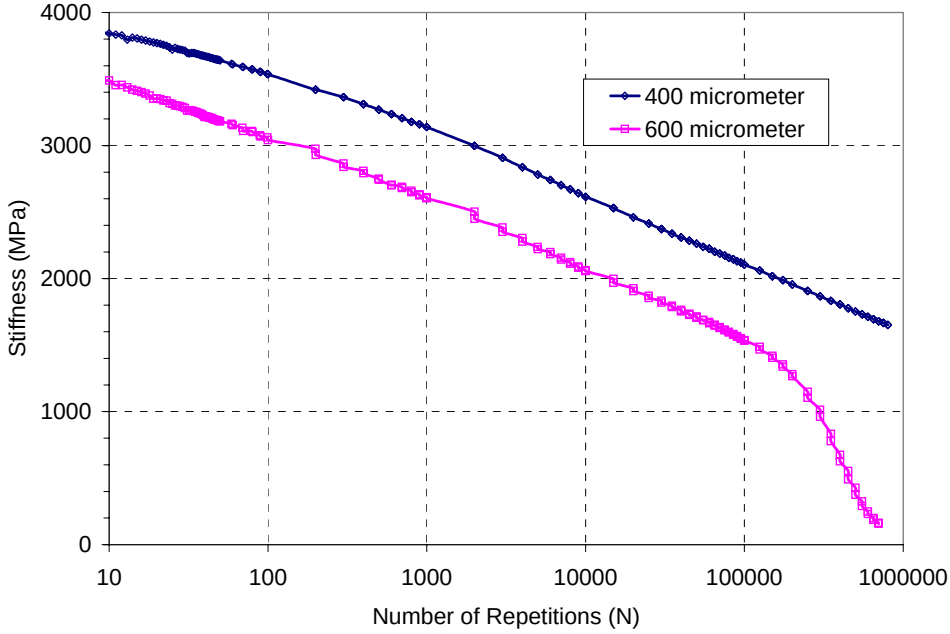

a) Stiffness

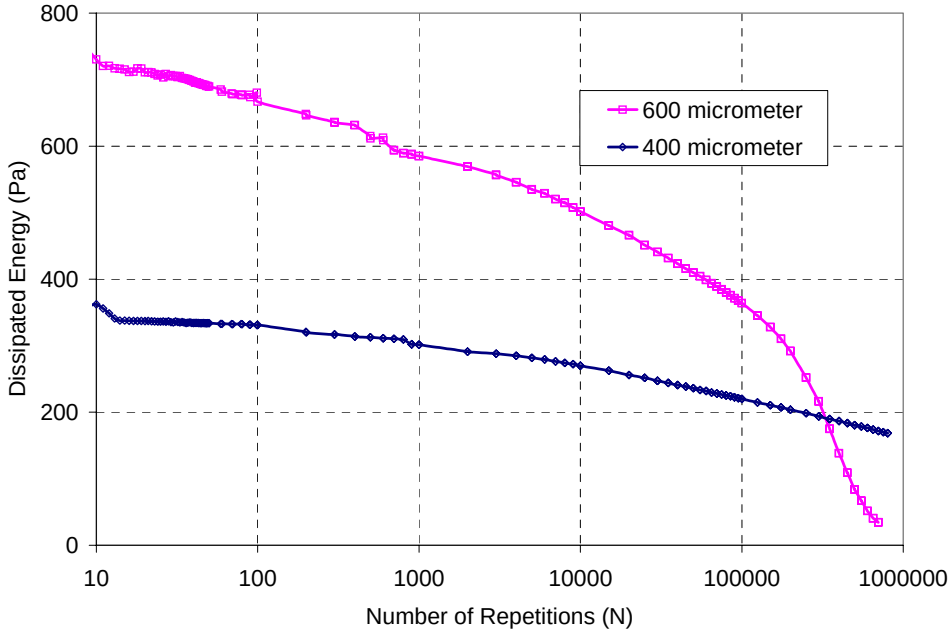

b) Dissipated Energy

Figure 4-4 Stiffness and Dissipated Energy vs. Number of Repetitions for MB-D Mix

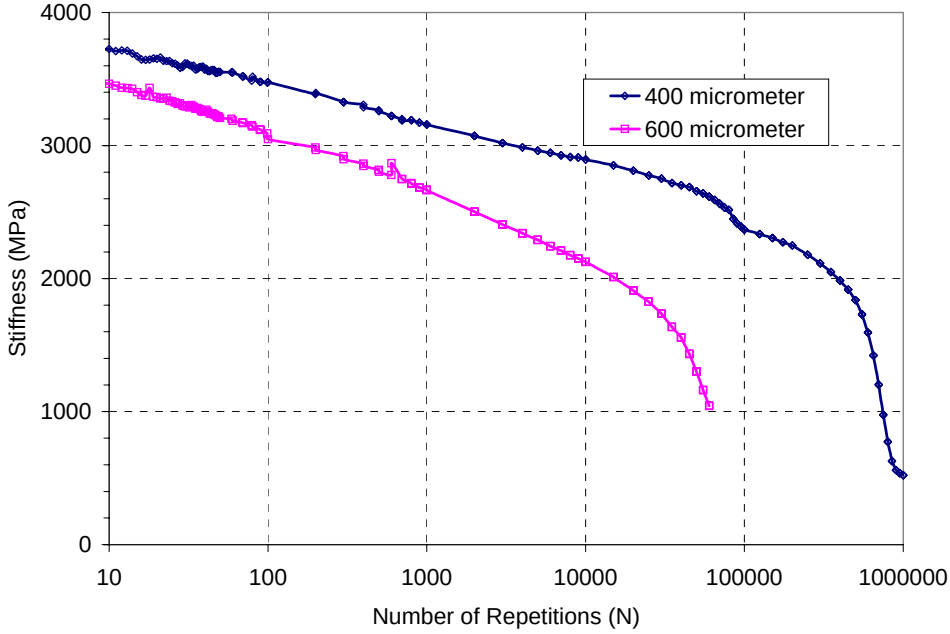

a) Stiffness

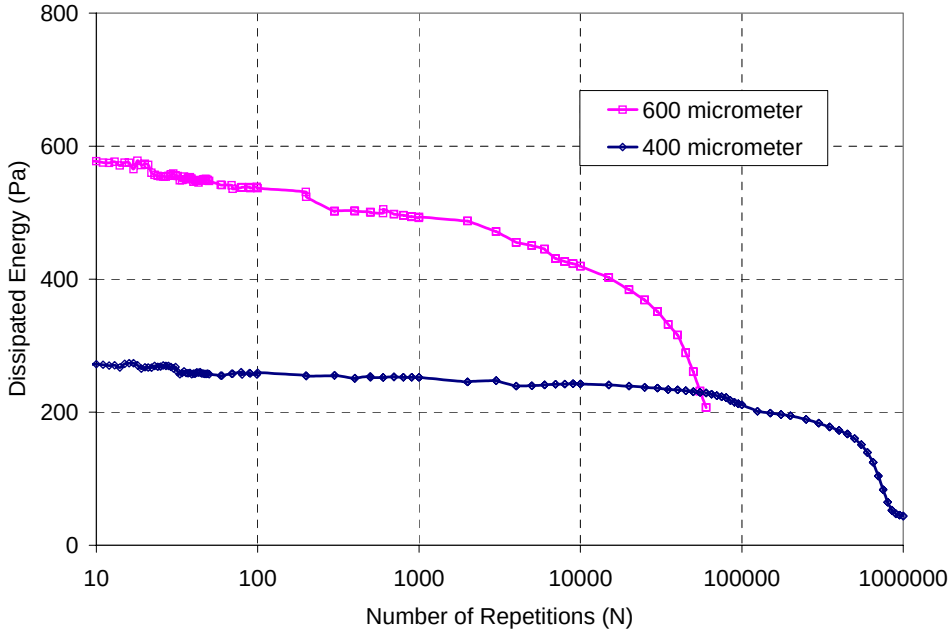

b) Dissipated Energy

Figure 4-5 Stiffness and Dissipated Energy vs. Number of Repetitions for DGAC Mix

Table 4-1 Summary of Fatigue Test Results

Sample ID	Avg. Air Voids, (%)	Average Strain (με)	Initial Stiffness (MPa)	Failure N_{f50}	Initial Phase Angle	Phase Angle @ N_{f50}	Test Temperature, °C		
							Min	Max	Avg
RAC-G (PES-1)									
3A	7.1	423	2,565	672,381	25.6	32.7	19.8	20.1	20.0
3B		430	2,826	239,217	25.3	33.2	19.9	19.9	19.9
4D		429	2,791	439,449	24.6	32.8	19.9	19.9	19.9
4A		649	1,972	62,645	28.7	35.1	19.9	20.4	20.2
4B		650	1,928	122,894	28.6	36.3	19.9	20.2	20.1
4C		643	2,467	24,464	27.3	33.6	19.9	20.0	20.0
RUMAC (PES-4)									
7A	4.5	434	3,029	543,891	27.8	35.9	19.9	20.1	20.0
7B		434	3,205	469,804	27.1	36.0	19.9	20.0	20.0
7C		430	2,854	245,330	28.9	33.8	19.9	20.0	20.0
6B	4.7	644	2,645	141,093	30.1	37.5	19.9	20.0	19.9
6C		642	2,947	168,058	31.1	38.8	19.9	20.0	19.9
6D		637	2,874	135,946	32.2	38.9	19.9	20.0	20.0
MB-G (PES-6)									
12C	1.9	424	2,755	1,167,669	43.9	50.8	19.9	20.0	20.0
12F		419	2,666	1,455,841	44.4	51.1	19.9	20.0	19.9
12E		425	3,739	340,383	38.6	47.7	19.9	19.9	19.9
10C	3.7	630	2,290	286,599	48.1	53.7	19.9	20.2	20.0
12A	1.9	627	2,470	256,808	47.2	53.5	19.9	20.0	19.9
12B[1]		630	2,151		48.2		19.9	21.9	21.0
MB-D (PES-7)									
14A	3.9	427	3,536	332,294	39.4	47.6	19.9	20.0	20.0
14B		427	3,568	429,722	39.6	47.6	19.9	20.0	20.0
14C		428	3,816	356,036	40.1	48.9	19.9	20.0	19.9
14D		628	3,180	80,359	45.2	52.7	19.9	20.1	20.0
15A	3.6	635	3,126	63,450	42.5	50.8	19.9	20.0	20.0
15B		626	3,237	108,300	43.8	51.6	19.9	20.0	19.9
DGAC (PES-9)									
19A[2]	6.8	424	2,361		34.6		20.1	20.7	20.5
19B		429	3,304	621,980	32.8	39.7	19.5	20.3	19.9
19C		423	3,802	410,847	30.3	38.5	20.0	20.1	20.0
19D		630	3,316	79,372	33.2	41.4	20.0	20.2	20.1
20A		627	3,039	23,116	34.1	42.1	20.0	20.5	20.4
20B		629	3,264	39,623	32.3	40.8	19.9	20.0	20.0

[1] Stiffness is not decreasing. Temperature issue. [2] Sample damaged

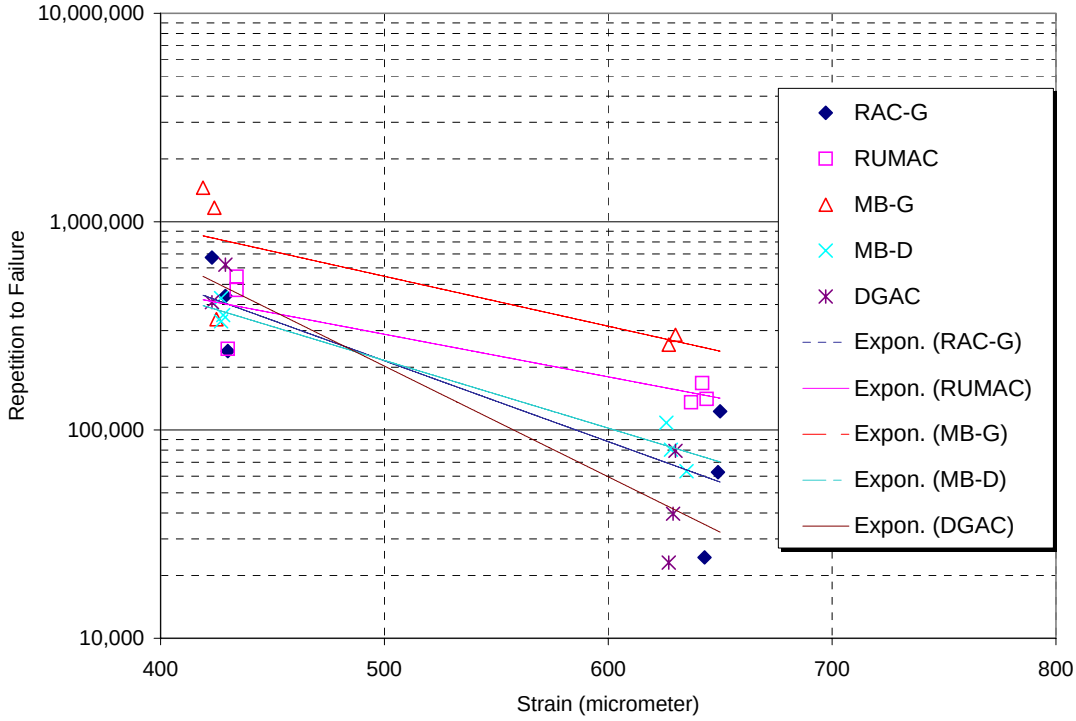

Figure 4-6 Repetitions to Failure vs. Strain for All Mixes

Table 4-2 Relationships between Repetitions to Failure and Strain

Mix	Repetitions to Failure	R^2
RAC-G	$9E+07e^{-0.0089(\varepsilon)}$	0.7533
RUMAC	$3E+06e^{-0.0047(\varepsilon)}$	0.7804
MB-G	$9E+06e^{-0.0055(\varepsilon)}$	0.5645
MB-D	$9E+06e^{-0.0075(\varepsilon)}$	0.9594
DGAC	$9E+07e^{-0.0122(\varepsilon)}$	0.8882

ε = strain in micrometer.
e = exponential constant (2.71828)

4.1.3 Initial Stiffness and Dissipated Energy

Figure 4-7 shows a comparison of initial stiffness while Figure 4-8 shows a comparison of dissipated energy for all mixes at two strain levels.

The MB-D mix had the highest average initial stiffness of all mixes, while the RAC-G mix had the lowest average initial stiffness, and the MB-G mix had the largest variation in initial stiffness. The dissipated energy is obviously a function of strain as shown in Figure 4-8: the higher the strain the larger the dissipated energy. It also appears that dissipated energy is a function of stiffness: as the stiffness increases, the dissipated energy increases.

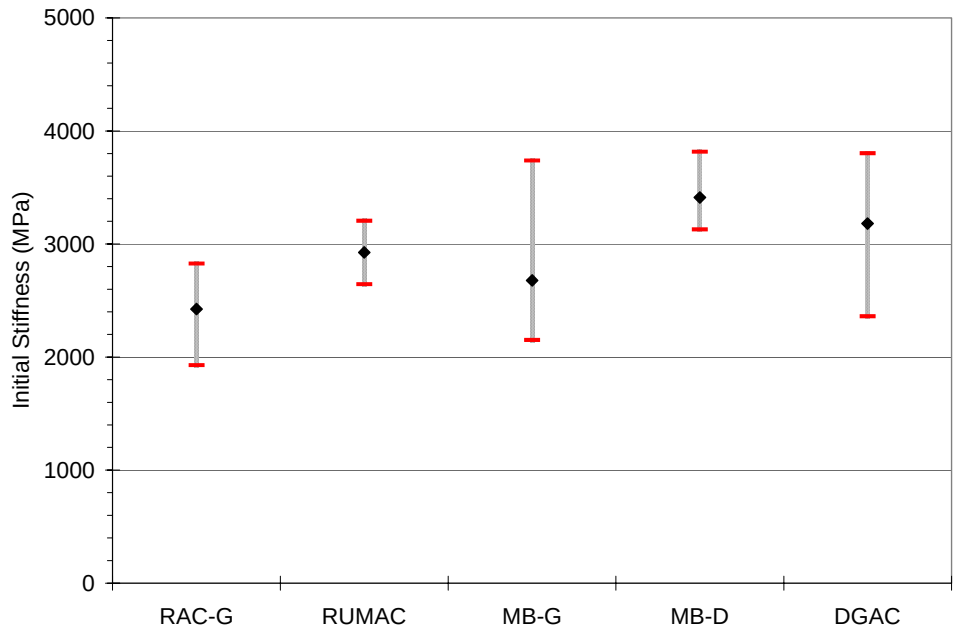

Figure 4-7 Comparison of Initial Stiffness among Mixes

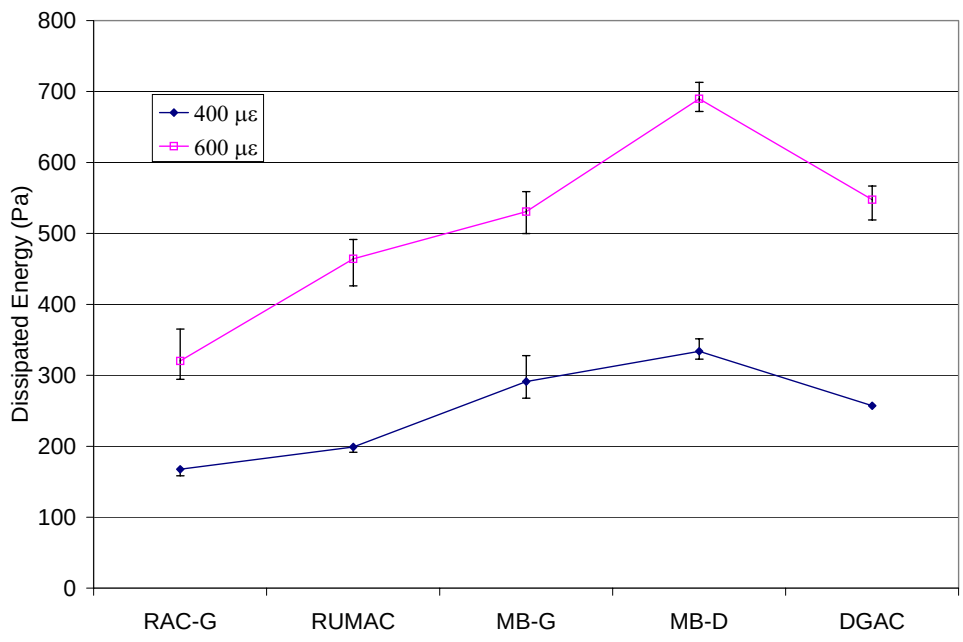

Figure 4-8 Comparison of Dissipated Energy among Mixes

4.2 RELATIVE FATIGUE PERFORMANCE OF MIXES

A simple method was used to rank the relative fatigue performance of the mixes. The method is based on a 1 to 5 scale with 5 being the best. Table 4-3 provides a summary of this ranking for each mix type. The summary indicates the fatigue performance of the mixes is influenced by the testing strain level. Overall, the MB-G mix had the highest total score, indicating the mix was the best in fatigue performance. The RAC-G and RUMAC mixes ranked next while the MB-D and DGAC mixes were worst among the mixes tested.

Table 4-3 Relative Fatigue Performance Ranking

Mix Type	Approximate Strain Level		Total Score
	400 με	600 με	
RAC-G	4	2	6
RUMAC	2	4	6
MB-G	5	5	10
MB-D	1	3	4
DGAC	3	1	4

5.0 HAMBURG WHEEL TRACKING TEST

The Hamburg Wheel Tracking test was performed in accordance with AASHTO T324-04 [AASHTO, 2004c] *Standard Method of Test for Hamburg Wheel-Track Testing of Compacted Hot-Mix Asphalt (HMA)*. This method provides a means to evaluate the rutting potential of hot-mix asphalt samples due to a weakness in the aggregate structure, inadequate binder stiffness, or moisture damage. The moisture-susceptibility of HMA can be evaluated since the specimens are submerged in temperature-controlled water during loading. The test also provides information about the rate of permanent deformation from a moving concentrated load.

The test was conducted on pavement cores (DGAC mix only) and field-mixed field-compacted (FMFC) and field-mixed lab-compacted (FMLC) specimens for the rubber modified mixes. The FMLC specimens were made from loose mixes obtained during the construction. Table 5-1 shows the samples used in the test. All tests were performed at 50°C.

Table 5-1 Samples Used in Hamburg Wheel Tracking Test

Compaction Method	Sample Type	Mix Type	Number of Samples
FMFC	Core	DGAC	8 (16 cores)
FMFC	Slab	RAC-G RUMAC MB-G MB-D DGAC	2 for each mix
FMLC	Slab	RAC-G RUMAC MB-G MB-D	4 for RUMAC 2 for other mixes

5.1 FIELD-MIXED FIELD-COMPACTED CORE SAMPLES

Sixteen 150-mm DGAC cores were tested in the Hamburg Wheel Tracking device. Table 5-2 presents the measured rut depths at 10000 and 20000 wheel passes from each specimen along with other key test parameters. Figure 5-1 illustrates graphically the definition of stripping inflection point, inverse creep slope, and inverse tripping slope. Figures 5-2 through 5-4 show the progression of average deformation for these samples. Regression equations used to determine the inflection point, inverse creep slope, and inverse stripping slope are also shown in the figures. Appendix D provides graphs showing average deformation at various wheel positions.

During testing, the cores generally exhibited a large amount of deformation after 20000 passes. Significant loss of fines in the wheel path was observed as was bare aggregate.

Table 5-2 Summary of Hamburg Test Results from the Field Cores (DGAC Mix)

Core ID	Air Voids, %	Stripping Inflection Point (passes)	Inverse Creep Slope (pass/mm)	Inverse Stripping Slope (pass/mm)	Rut Depth @10000 passes (mm)	Rut Depth @20000 passes (mm)
L1-7, L1-8	5.3, 5.6	5693	2000	1000	8.34	15.95
L1-9, L1-10	5.7, 5.8	9882	2500	1000	6.05	17.12
L2-7, L2-8	5.4, 5.0	14849	3333	2000	5.33	9.20
L2-9, L2-10	5.5, 5.7	13771	2500	2000	6.26	11.32
L3-7, L3-8	5.6, 5.6	Data not saved				16.93
L3-9, L3-10	5.9, 6.2					6.73
L4-8, L4-9	3.1, 3.6	12910	5000	1429	4.53	15.97
L4-7, L4-10	3.8, 3.8	8205	5000	1000	3.75	9.97
Average		10885	3389	1405	5.71	12.90

- Inflection point is the number of wheel passes at the intersection of the creep slope and stripping slope and at which moisture damage starts to dominate performance.
- Inverses creep slope is used to measure rutting susceptibility and is reported in number of wheel passes per 1-mm.
- Inverse stripping slope is proportional to the rate of deformation (wheel passes per 1-mm rut depth) after the stripping inflection point.

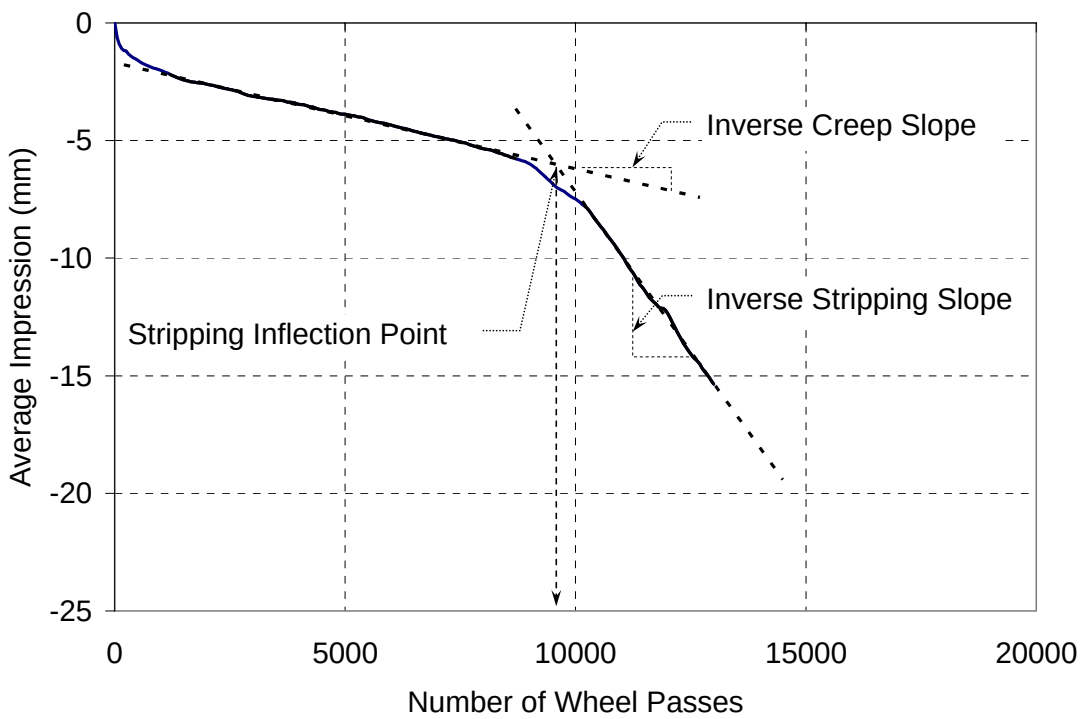

Figure 5-1 Illustration of Various Terms Used to Analyze the Hamburg Test Results

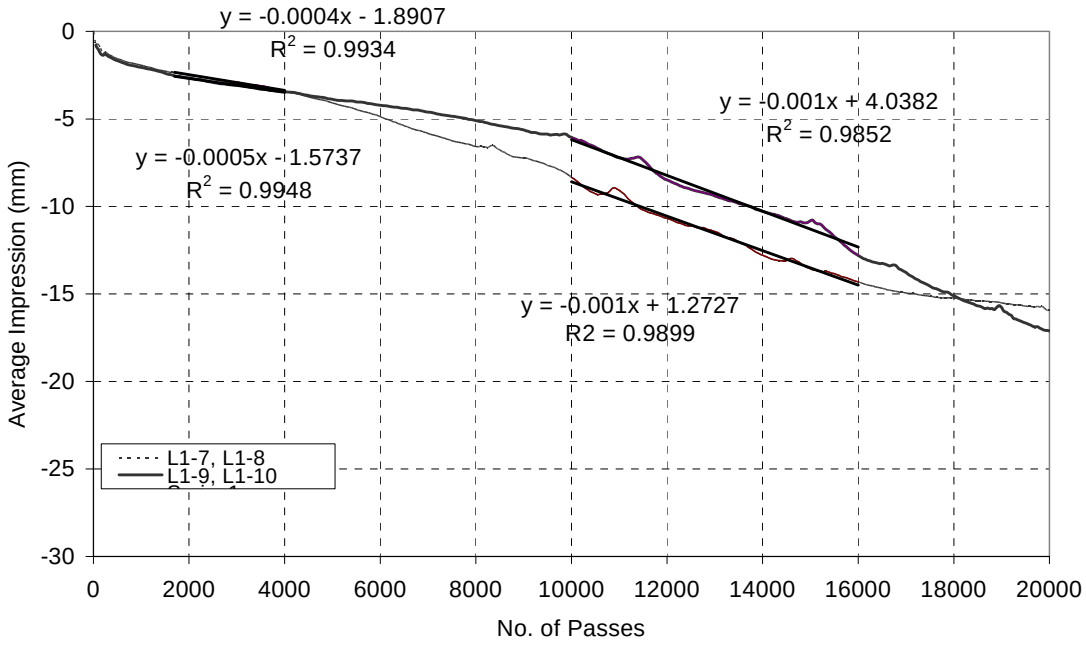

Figure 5-2 Progression of Average Deformation for Cores Taken at Stat132 L1 - DGAC Mix

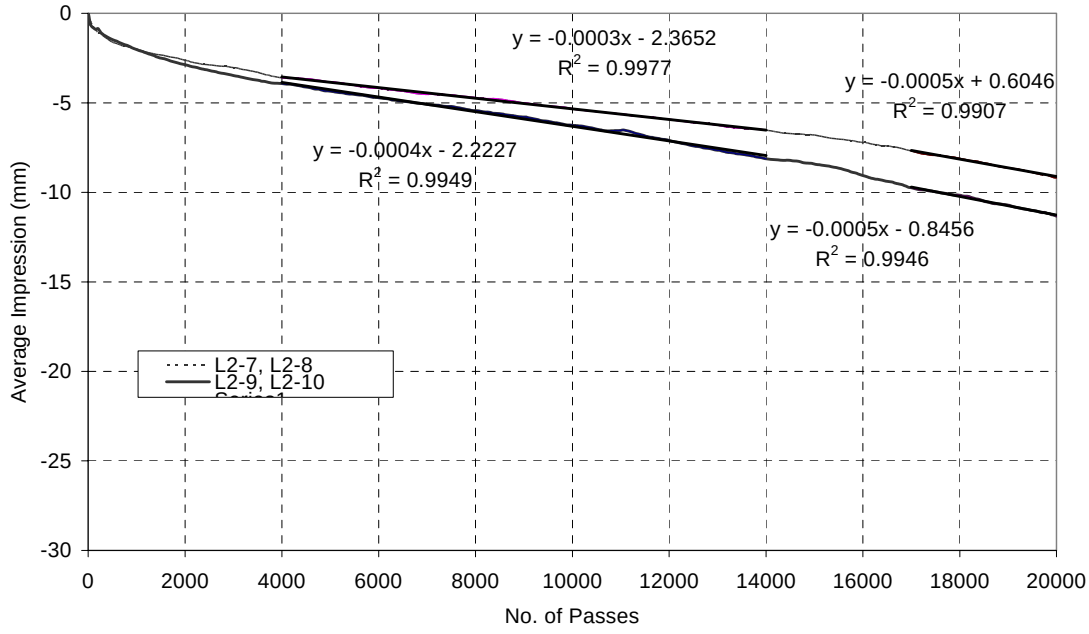

Figure 5-3 Progression of Average Deformation for Cores Taken at Stat132 L2 – DGAC Mix

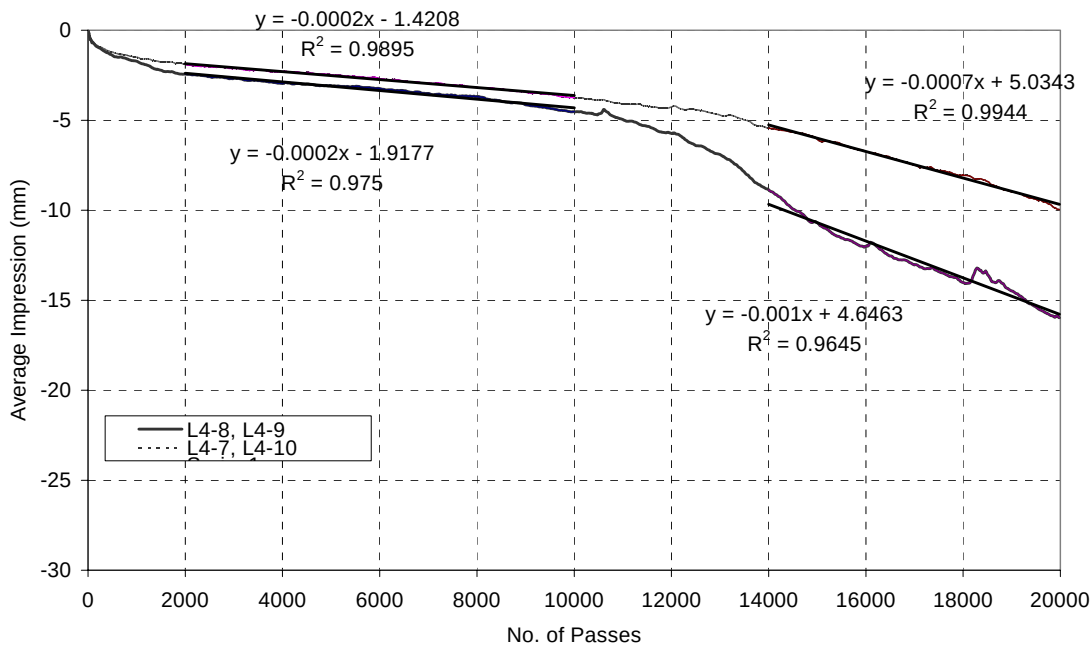

Figure 5-4 Progression of Average Deformation for Cores Taken at Stat132 L4 – DGAC Mix

5.2 FIELD-MIXED FIELD-COMPACTED SLAB SPECIMENS

5.2.1 Test Results from FMFC Slab Specimens

Table 5-3 presents the measured rut depths at 10000 and 20000 wheel passes from each specimen along with other key test parameters. Figures 5-5 through 5-9 show the progression of average deformation of different mixes tested. Rut depth at 20000 load cycles for the RAC-G, MB-G and MB-D mixes was predicted based on the stripping slope. During the testing, it was observed that all mixes showed significant rutting and loss of fines.

Table 5-3 Summary of Hamburg Test Results from the FMFC Slab Specimens

Mix Type	Air Voids, %	Stripping Inflection Point (passes)	Inverse Creep Slope (pass/mm)	Inverse Stripping Slope (pass/mm)	Rut Depth @10000 passes (mm)	Rut Depth @20000 passes (mm)
RAC-G-2	6.2	13912	5000	345	3.84	22.19*
RAC-G-3	7.0	9495	2500	385	7.48	32.82*
Average	**6.6**	**11704**	**3750**	**365**	**5.66**	**27.50**
RUMAC-6A	5.0	12815	3333	625	4.86	17.38*
RUMAC-6B	5.4	12308	10000	1667	3.64	8.24
Average	**5.2**	**12561**	**6667**	**1146**	**4.25**	**12.81**
MB-G-11	1.4	7506	1250	303	14.65	47.81*
MB-G-2	3.8	10771	2000	278	6.86	39.75*
Average	**2.6**	**9138**	**1625**	**290**	**10.76**	**43.78**
MB-D-13	4.6	9881	3333	1000	4.76	14.44*
MB-D-14	2.6	2825	1429	625	13.90	29.90*
Average	**3.6**	**6353**	**2381**	**813**	**9.33**	**22.17**
DGAC17	4.9	12479	3333	769	4.28	13.79
DGAC20	7.1	6189	2500	1667	6.95	13.38
Average	**6.0**	**9334**	**2917**	**1218**	**5.62**	**14.06**

* Predicted

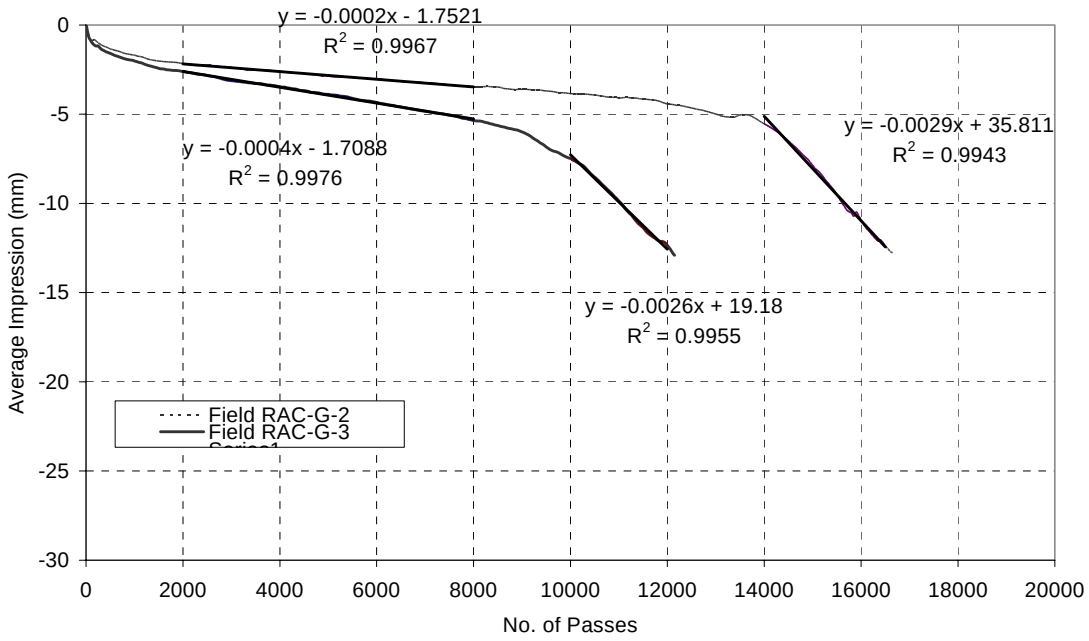

Figure 5-5 Progression of Average Deformation for Field Mixed Field Compacted RAC-G Mix

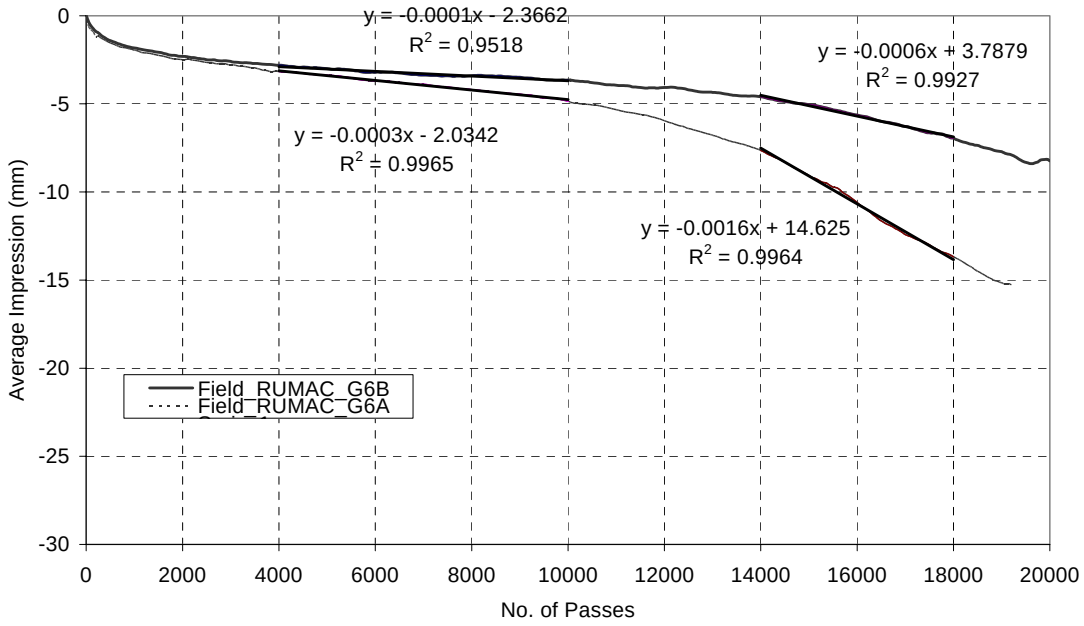

Figure 5-6 Progression of Average Deformation for Field Mixed Field Compacted RUMAC Mix

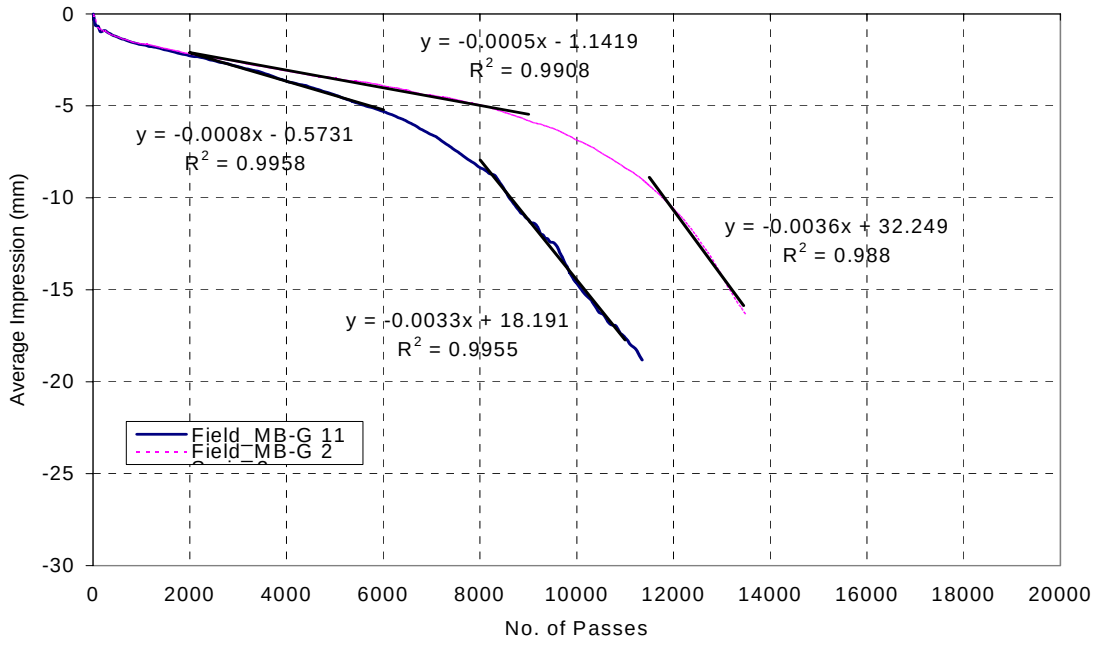

Figure 5-7 Progression of Average Deformation for Field Mixed Field Compacted MB-G Mix

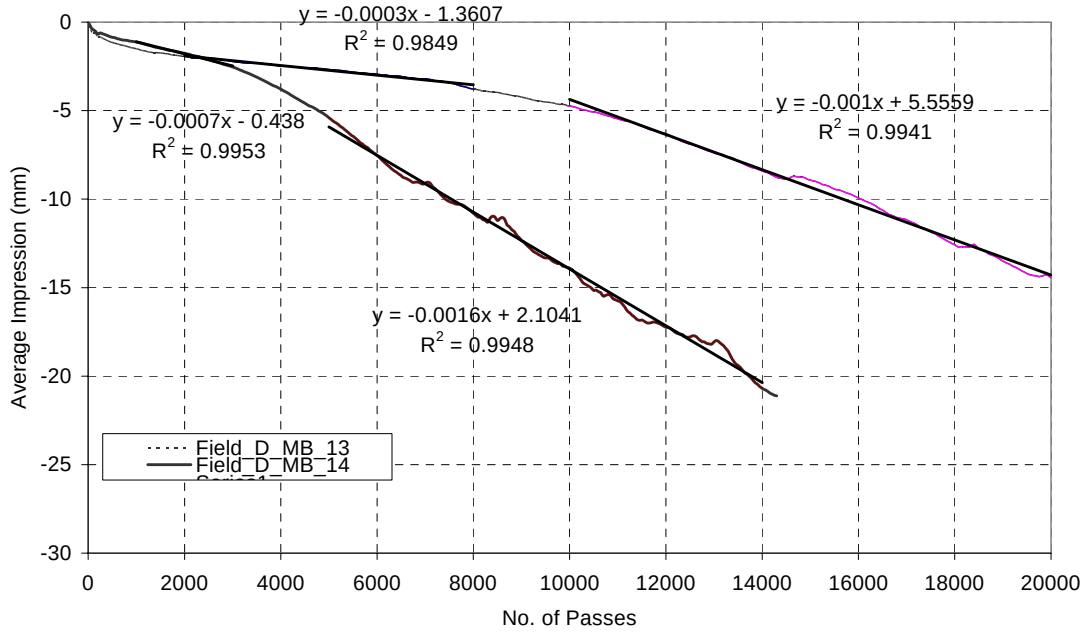

Figure 5-8 Progression of Average Deformation for Field Mixed Field Compacted MB-D Mix

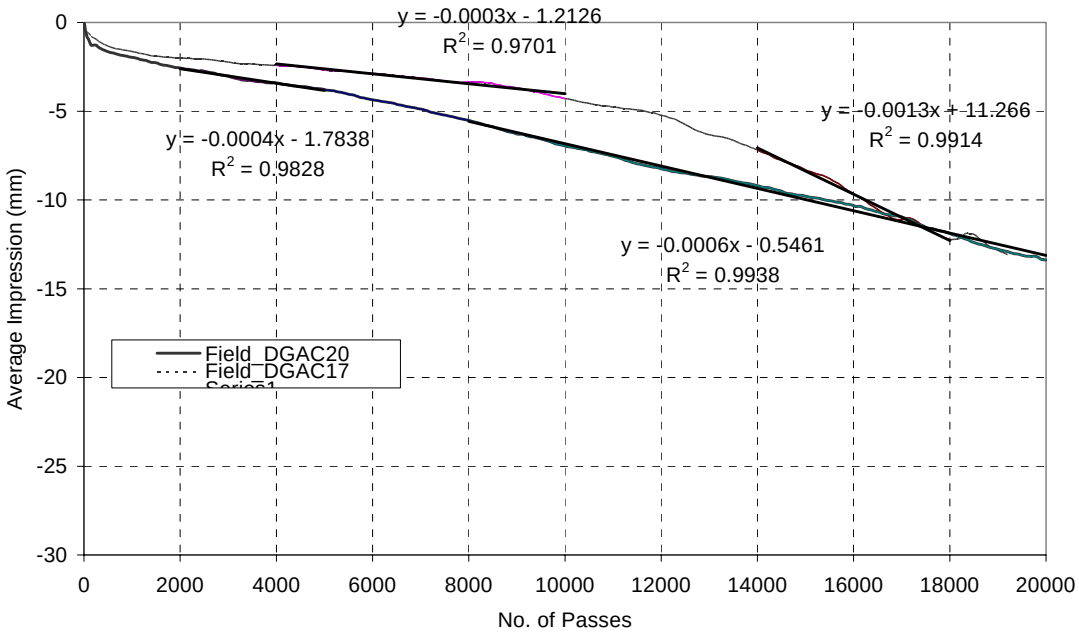

Figure 5-9 Progression of Average Deformation for Field Mixed Field Compacted DGAC Mix

5.2.2 Performance Comparison for FMFC Slab Specimens

Figure 5-10 shows the variation of measured rut depth at 10000 and 20000 load cycles for FMFC specimens. A comparison of average rut depth is also shown in Figure 5-11. Both figures indicate that the MB-G mix is most susceptible to rutting compared to other mixes tested while RUMAC is the least. Bleeding on the MB-G sections, observed during the field visit, is consistent with the lab test results.

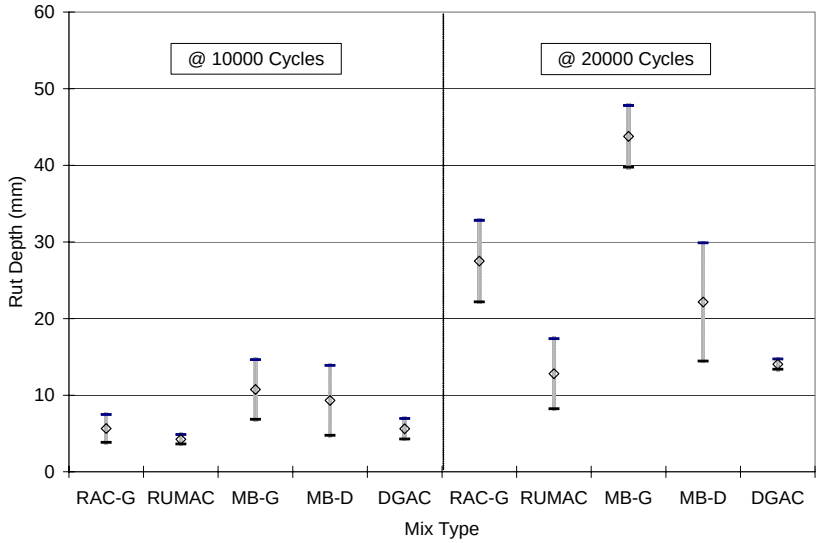

Figure 5-10 Variation of Measured Rut Depth at 10000 and 20000 Load Cycles for FMFC Mixes

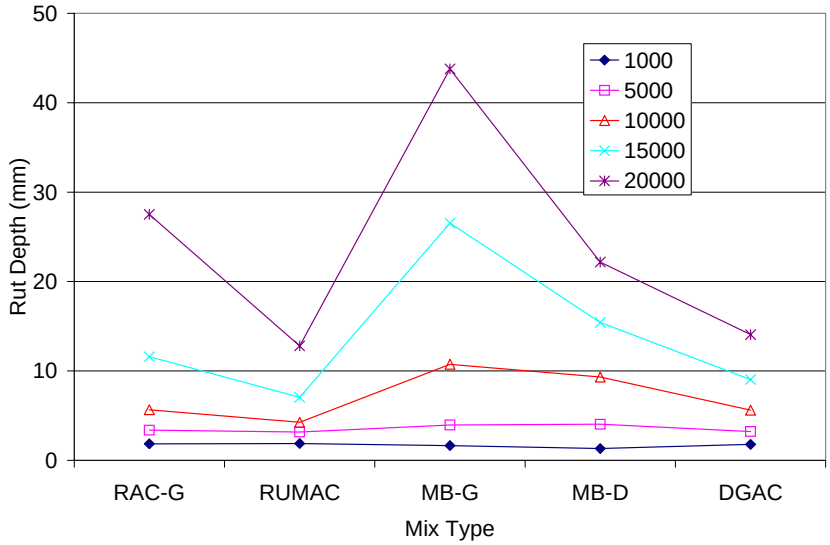

Figure 5-11 Comparison of Average Rut Depth for Field Mixed Field Compacted Mixes

Note that the Hamburg test also allows evaluation of moisture-susceptibility of HMA by analyzing the progression of the deformation through the following parameters: inflection point; inverse creep slope and inverse stripping slope. These parameters were previously defined in Figure 5-1. A mix with a higher inflection point and inverse creep slope is less susceptible to rutting. A mix with higher inverse stripping slope indicates that the mix would have a slower rate of moisture damage once the moisture damage becomes the dominate mode of failure.

Comparisons of inflection point, inverse creep slope, and inverse stripping slope among mixes are presented in Figure 5-12. The data indicate that the RUMAC mix was the most rut resistant and the MB-G the least. The data also indicate that the RUMAC mix was the most resistant to moisture damage; the MB-G and MB-D were the least resistant to moisture damage. Overall, the RUMAC mix performed the best in the Hamburg wheel tracking while the MB-G mix performed the worst.

5.3 FIELD-MIXED LAB-COMPACTED SLAB SPECIMENS

5.3.1 Test Results from FMLC Slab Specimens

Loose mixes of RAC-G, RUMAC, MB-G and MB-D obtained during the construction were compacted at 150°C in the University of California at Berkeley (UCB) laboratory with a rolling wheel compactor. No DGAC mix was obtained from the field. The target air void content for the specimens was 4±1%.

Table 5-4 presents the measured rut depths at 10000 and 20000 wheel passes from each specimen. Figures 5-13 through 5-17 illustrate the progression of average deformation of the samples. Note that the specimens showed a greater deformation after 20000 wheel passes for the RAC-G, MB-G, and MB-D mixes, than for RUMAC. Significant loss of fines and bare aggregate were observed for the RAC-G and MB-D mixes; loss of fines from the MB-G and RUMAC mixes was less noticeable.

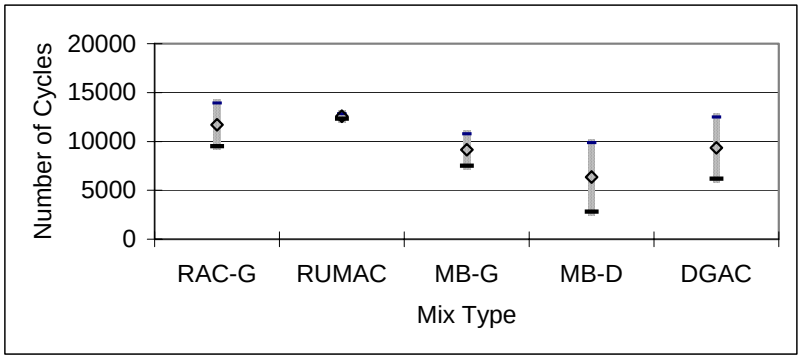

Inflection Point

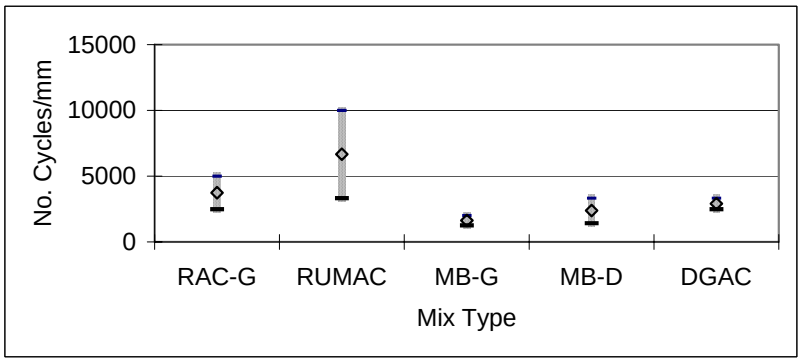

Inverse Creep Slope

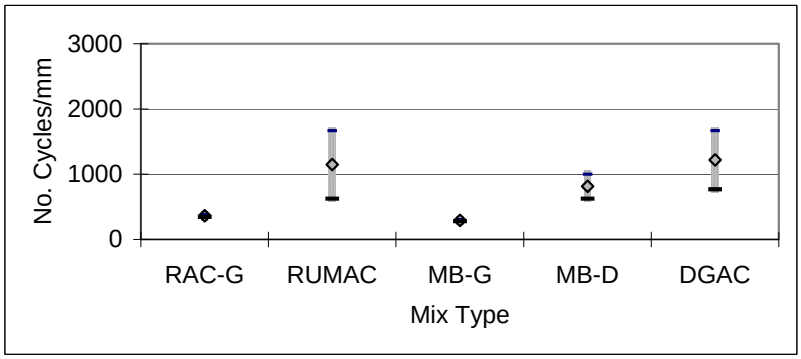

Inverse Stripping Slope

Figure 5-12 Inflection Point, Inverse Creep Slope, and Inverse Stripping Slope for FMFC Mixes

Table 5-4 Summary of Hamburg Test Results from FMLC Slab Specimens

Mix Type	Air Voids, %	Stripping Inflection Point (passes)	Inverse Creep Slope (pass/mm)	Inverse Stripping Slope (pass/mm)	Rut Depth @10000 passes (mm)	Rut Depth @20000 passes (mm)
RAC-G-1A	6.4	4461	2000	1250	8.16	17.64
RAC-G-1B	6.9	6428	2000	769	10.76	23.22*
Average	**6.6**	**5445**	**2000**	**1010**	**9.45**	**20.43**
RUMAC-1A	5.9	Unidentifiable			3.26	4.25
RUMAC-1B	5.8	14619	5000	2500	4.41	7.04
RUMAC-2A	4.7	Unidentifiable			3.76	5.39
RUMAC-2B	4.3	12802	5000	2000	3.98	9.07
Average	**5.2**	**13710**	**5000**	**2250**	**3.85**	**6.44**
MB-G-1A	6.1	Unidentifiable			16.21	24.47*
MB-G-1B	5.4	12365	1667	714	12.04	24.04*
Average	**5.8**	**12365**	**1667**	**714**	**14.13**	**24.26**
MB-D-1A	6.2	7783	1250	909	12.22*	23.48*
MB-D-1B	5.9	5946	1250	476	16.96*	37.62*
Average	**6.1**	**6865**	**1250**	**693**	**14.59**	**30.55**

* Predicted.

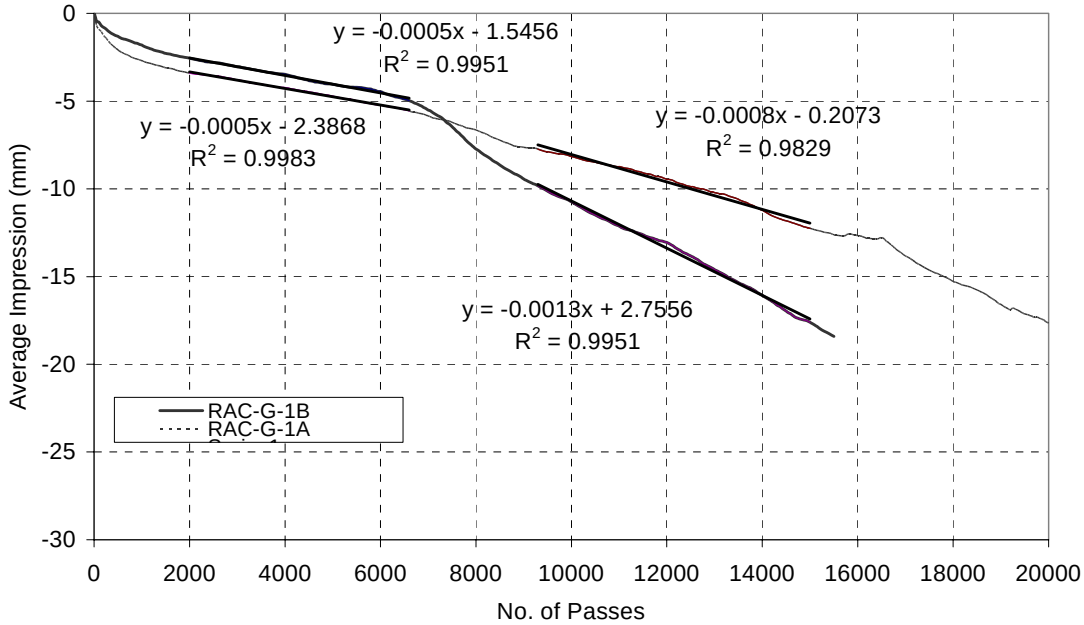

Figure 5-13 Progression of Average Deformation for Field Mixed Lab Compacted RAC-G Mix

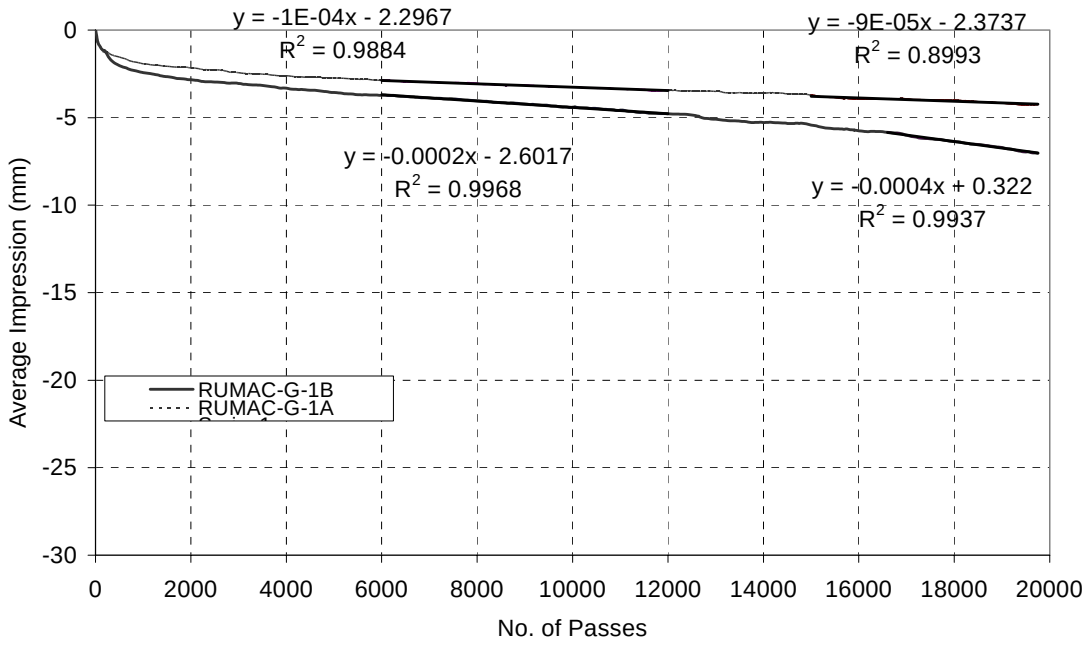

Figure 5-14 Progression of Average Deformation for Field Mixed Lab Compacted RUMAC Mix-1

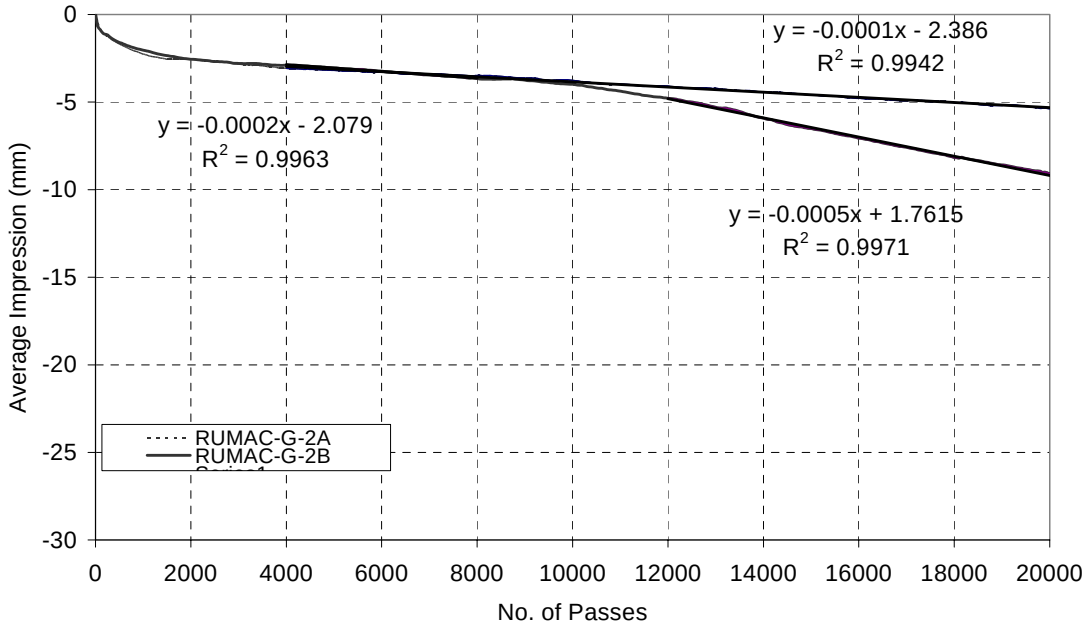

Figure 5-15 Progression of Average Deformation for Field Mixed Lab Compacted RUMAC Mix-2

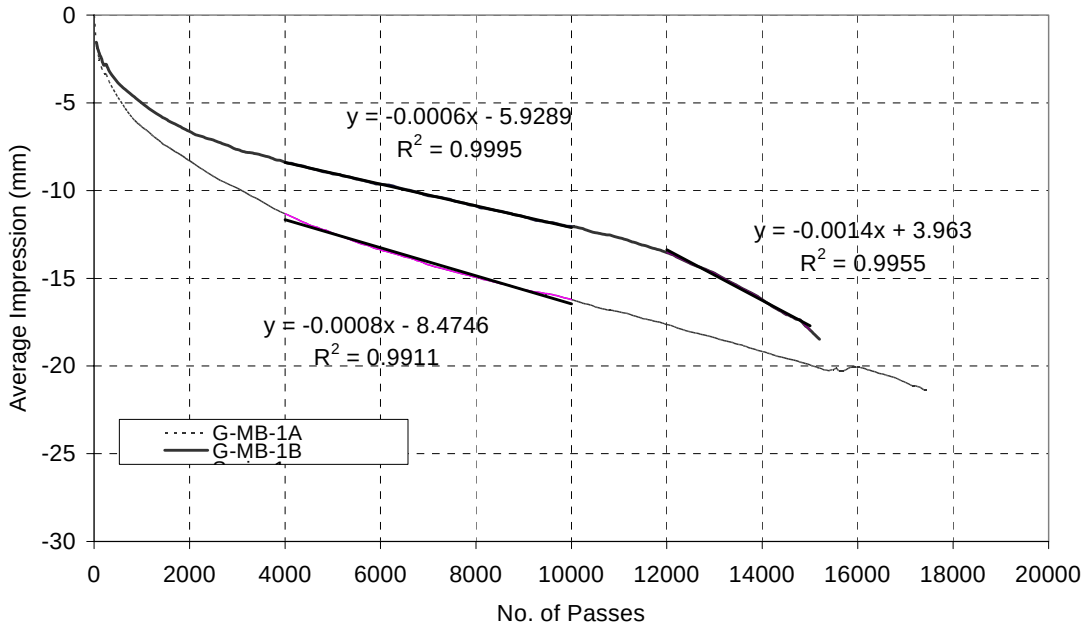

Figure 5-16 Progression of Average Deformation for Field Mixed Lab Compacted MB-G Mix

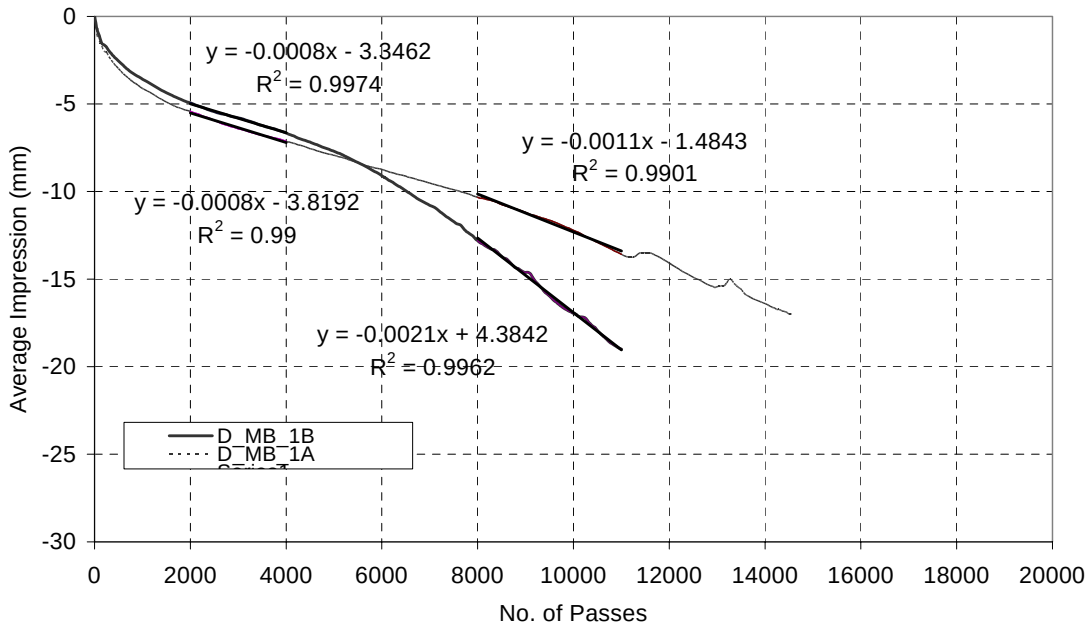

Figure 5-17 Progression of Average Deformation for Field Mixed Lab Compacted MB-D Mix

5.3.2 Performance Comparison for FMLC Slab Specimens

Figure 5-18 shows a variation of measured rut depth at 10000 and 20000 load cycles for all FMLC specimens. A comparison of average rut depth is shown in Figure 5-19. Both figures indicate that among the four FMLC mixes, the RUMAC mix is least susceptible to rutting and the MB-D mix is most.

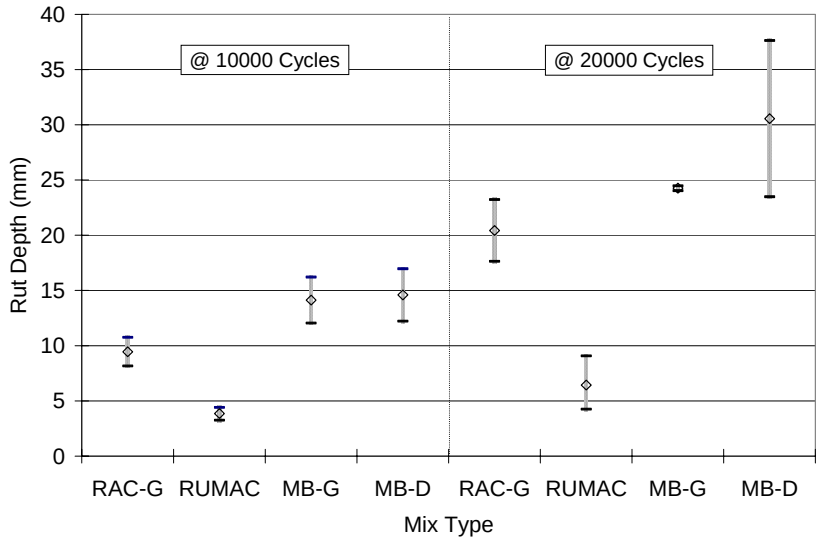

Figure 5-18 Variation of Measured Rut Depth at 10000 and 20000 Load Cycles for FMLC Mixes

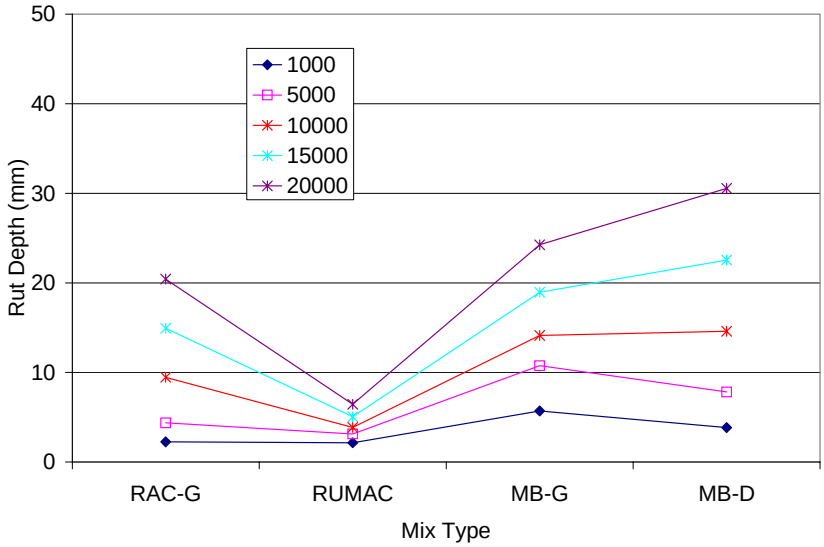

Figure 5-19 Comparison of Average Rut Depth for Field Mixed Lab Compacted Mixes

The susceptibility to rutting and moisture damage can also be indicated by the inflection point and the inverse creep slope. As shown in Figure 5-20, the data indicate that the RUMAC mix was the most rut resistant and the MB-D mix the least. Also, the data indicate the RUMAC mix was the most resistant to moisture damage whereas the MB-G and MB-D were the least. Overall, the RUMAC mix consistently performed the best, and the MB-D the worst.

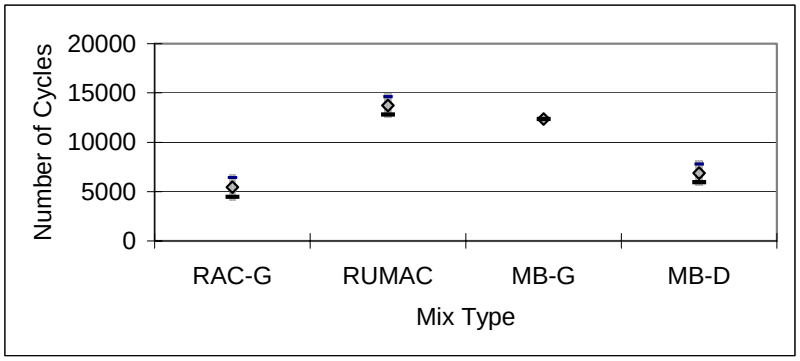

Inflection Point

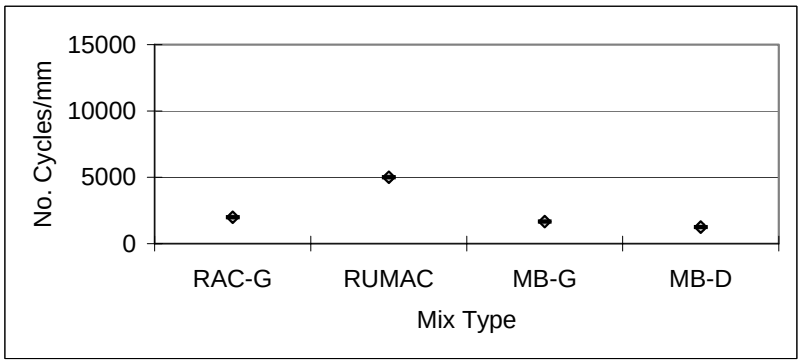

Inverse Creep Slope

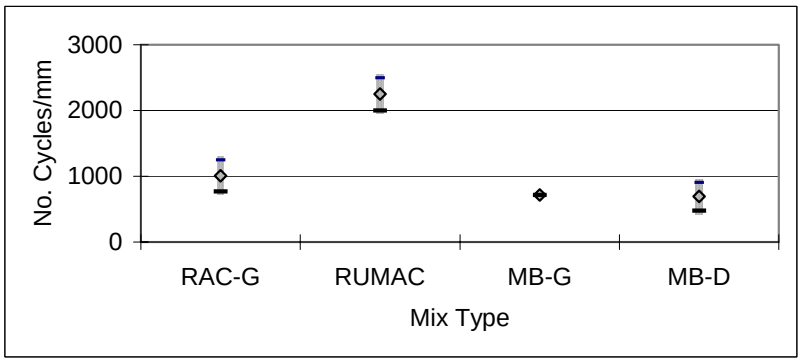

Inverse Stripping Slope

Figure 5-20 Inflection Point, Inverse Creep Slope, and Inverse Stripping Slope for FMLC Mixes

5.4 COMPARISON OF FMFC AND FMLC SLAB SPECIMENS

5.4.1 Comparison of Measured Rut Depth

A comparison of measured rut depth from specimens made from FMFC and FMLC materials, as shown in Figure 5-21, indicates that the test results are generally comparable. The lab compacted mixes showed slightly higher rutting, suggesting that the aging effect during mix production is less pronounced in the lab compacted mixes than that of the field compacted mixes.

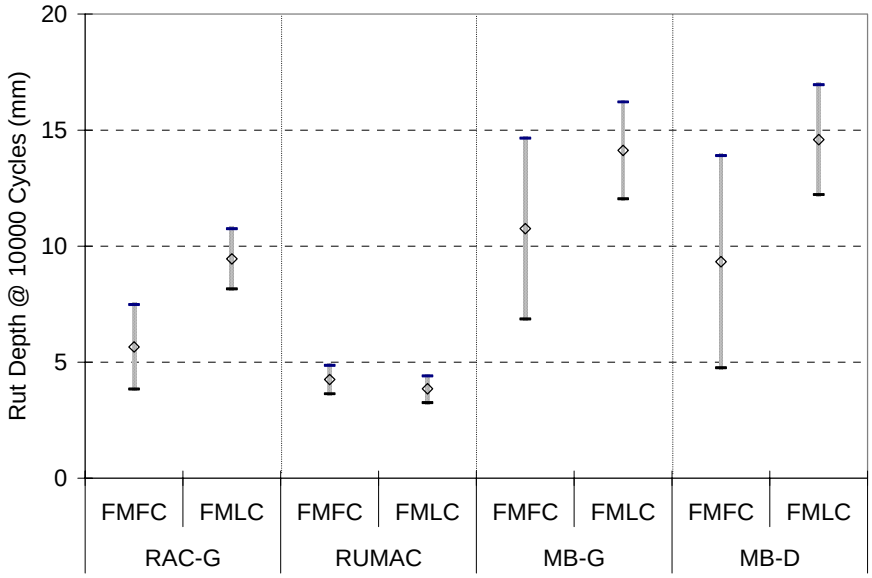

Figure 5-21 Comparison of Measured Rut Depth between FMFC and FMLC Specimens

5.4.2 Effect of Air Void Content on Rutting

Data from both the FMFC and FMLC specimens were combined to develop Figure 5-22 which shows relationships between measured rut depth and air void content for all mixes. The figure indicates that the rutting performance of the MB-G and MB-D mixes is very sensitive to the amount of air voids in the mix. A small deviation from 4% air void content could result in poor rutting performance. The RUMAC mix appears to be least sensitive. When the air void content exceeds 6%, the RAC-G may perform poorly. The DGAC mix data indicate rut resistance decreases for air void content greater than 5%.

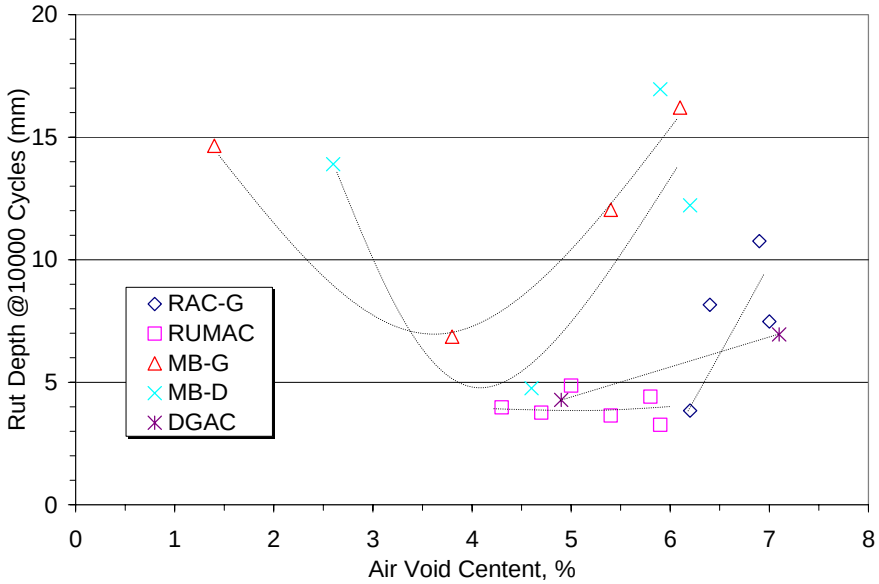

Figure 5-22 Measured Rut Depth vs. Air Void Content

5.5 RELATIVE PERFORMANCE IN HAMBURG WHEEL TRACK DEVICE

A simple method was used to rank the relative performance of the mixes. The method is based on a 1 to 5 scale with 5 being the best in the lab performance. Table 5-5 provides a summary of this ranking for each mix type. The summary indicates the RUMAC mix had best rutting performance and MB-G the worst. The summary also indicates the RUMAC mix had best performance in terms of resisting moisture damage; the MB-G and MB-D mixes performed poorly. Overall, the RUMAC mix was relatively the best performer. RAC-G and DGAC ranked next. The MB-G and MB-D mixes were worst among the mixes tested.

Table 5-5 Relative Performance Ranking in Hamburg Wheel Track Device

Mix Type	Performance Ranking for			Total Score
	Rutting	Initiation of Moisture Damage	Rate of Moisture Damage after Initiation	
RAC-G	4	4	2	10
RUMAC	5	5	4	14
MB-G	1	2	1	4
MB-D	2	1	3	6
DGAC	3	3	5	11

6.0 CONCLUSIONS AND RECOMMENDATIONS

6.1 CONCLUSIONS

This lab test report presents the results of rutting, fatigue and wheel tracking test. It appears that no single mix performed consistently in the various tests; i.e., performance of the mixes was test-dependant. Table 6-1 presents a summary of performance ranking for each mix type.

Table 6-1 Summary of Performance Ranking

Mix Type	Rutting Performance				Fatigue Performance			Hamburg Wheel Tracking Test			
	40°C	50°C	60°C	Total Score	400 με	600 με	Total Score	Rutting (50°C)	Initiation of Moisture Damage (MD)	Rate of MD after Initiation	Total Score
RAC-G	3	4	3	10	4	2	6	4	4	2	10
RUMAC	2	5	2	9	2	4	6	5	5	4	14
MB-G	1	3	4	8	5	5	10	1	2	1	4
MB-D	5	2	5	12	1	3	4	2	1	3	6
DGAC	4	1	1	6	3	1	4	3	3	5	11

The following conclusions can be drawn based on the overall mix performance in the laboratory tests:

- Rutting Performance – Based on the results from both the SST and Hamburg Wheel Tracking tests, the RUMAC and RAC-G were the best performers. MB-D ranked next while the MB-G and DGAC mixes were worst among the mixes tested.
- Fatigue Performance – The MB-G mix was the best performer. RAC-G and RUMAC ranked next while the MB-D and DGAC mixes were poorest among the mixes tested.
- Performance in the Hamburg Wheel Tracking Device – The RUMAC mix was the best performer. RAC-G and DGAC ranked next while the MB-G and MB-D mixes were worst among the mixes tested.

6.2 RECOMMENDATIONS

The cause of the bleeding in the MB-G sections should be investigated. Field cores should be obtained to determine binder content.

As noted in the report, the air void content greatly affected the rutting performance. Caltrans should consider conducting additional SST and Hamburg wheel tracking tests on specimens made with different air void contents. The specimens can be prepared in the laboratory using available materials from the project. The test results may be useful to indicate if there is a need to revisit field density requirements during the construction.

Based on the laboratory test results, all asphalt-rubber modified mixes (except for MB-G in rutting performance) performed at least equally well as, if not better than, the conventional DGAC mix; therefore, the asphalt-rubber modified mixes should continue to be used in applications that are most cost effective.

7.0 REFERENCES

AASHTO, 2004a. "Standard Method of Test for Determining the Permanent Shear Strain and Stiffness of Asphalt Mixtures Using the Superpave Shear Tester (SST)," AASHTO Designation: T320-03, American Association of State Highway and Transportation Officials, Washington, D.C., 2004

AASHTO, 2004b. "Standard Method of Test for Determining the Fatigue Life of Compacted Hot-Mix Asphalt (HMA) Subjected to Repeated Flexural Bending," AASHTO Designation: T321-03, American Association of State Highway and Transportation Officials, Washington D.C., 2004.

AASHTO, 2004c. "Standard Method of Test for Hamburg Wheel-Track Testing of Compacted Hot-Mix Asphalt (MHA)," AASHTO Designation: T324-04, American Association of State Highway and Transportation Officials, Washington, D.C., 2004

Caltrans, 1999. "Manual of Test and Analysis Program for Evaluation of New Paving Materials," California Department of Transportation, Draft, Sacramento, California, August 1999.

Caltrans, 2005. "Rubberized Asphalt Concrete Firebaugh Project Volume 1 – Construction Report," METS, Caltrans, Sacramento, CA, March 2005.

MACTEC, 2005. "Firebaugh Field Activities," Project Memorandum Prepared for Caltrans, Sacramento, CA, June 2005.